SOME ASPECTS OF THE PETROLOGY AND GEOCHEMISTRY OF SELECTED FRESHWATER CARBONATES

By

WILLIAM RICHARD TRENT

Bachelor of Science

University of Missouri at Kansas City

Kansas City, Missouri

1976

Submitted to the Faculty of the Graduate College
of the Oklahoma State University
in partial fulfillment of the requirements
for the Degree of
MASTER OF SCIENCE
July, 1978

SOME ASPECTS OF THE PETROLOGY AND

GEOCHEMISTRY OF SELECTED

FRESHWATER CARBONATES

Thesis Approved:

R. N. Dawson
Thesis Adviser

Gary F. Stewart

Zuhair al-Shaieb

Norman N. Durham
Dean of the Graduate College

PREFACE

This study concerns itself with several suites of freshwater carbonates which are representative of similar depositional environments. Surface data obtained from vertical outcrop sampling and subsurface core data were both utilized in this investigation.

The writer wishes to thank Dr. R. Nowell Donovan, thesis adviser, for suggesting the problem and offering his expertise and support during the study. Advisory committee members, Dr. Gary F. Stewart and Dr. Zuhair Al-Shaieb, provided assistance in data processing and geochemical analysis. Thanks is also due to Dr. Alex R. Ross, who contributed technical advice and assisted in sample collection. The writer wishes to express his appreciation to Dr. Lester W. Reed of the Oklahoma State University Department of Agronomy for the use of the facilities of the soil preparation lab. Dr. Donald Holbert of the Oklahoma State University Department of Statistics deserves special recognition for his assistance in statistical analysis of the geochemical data. The faculty of the Oklahoma State University Department of Geology are also thanked for their helpful suggestions and criticisms during the writer's graduate career. Partial financial support was subsidized by an Arts and Sciences research grant awarded for the month of July, 1977.

Finally, the writer would like to express his sincere gratitude to his wife, Patricia, for her patience and understanding, and to his

parents and in-laws for their continued encouragement and financial support.

TABLE OF CONTENTS

Chapter Page

LIST OF TABLES

LIST OF FIGURES

Figure Page

CHAPTER I

INTRODUCTION

Purpose of Investigation

Freshwater carbonate sedimentation has received little attention by the geologic community. The reasons for this are two-fold. Foremost, small economic profit is inherent in freshwater carbonates. Secondly, because freshwater carbonates compose a minute section of the geologic record, interest in their composition and formation has been neglected by comparison with the study of marine carbonates.

The purpose of this study is to evaluate the geochemistry and petrology of selected freshwater carbonates. It is thought that a geochemical study of carbonates of this origin, particularly with regard to their mineralogy and trace element composition, will provide useful data for comparison with other areas where deposits of this type are found. In addition, it is hoped that the geochemical data attained will bolster our knowledge of carbonate sedimentation in different environments of deposition.

The present work is intended to complement the work of Armstrong (1978) which addresses similar deposits from different geographic locations.

Previous Work

Most previous work has concerned freshwater deposits of one type (e.g., tufas, speleothems, lacustrine deposits, caliches, hot spring deposits, etc.) from a single location, whereas this investigation involves a series of different freshwater carbonates from a variety of locations.

Literature review affords little detailed background information. Most pertinent has been the work of Müller (1969a, 1972) and his associates. Carbonate Sedimentology in Central Europe (ed. Müller and Friedman, 1968) summarizes previous work on freshwater carbonates and offers probably the most extensive bibliography available on the subject.

Kolesar's thesis (1968) discussed the mineralogy, geochemistry, and petrography of an assortment of freshwater carbonates and proposed the theory that this type may provide a clue as to whether or not marine carbonates have actually been cemented under terminal conditions of subaerial exposure to freshwater.

In his thesis, Herlinger (1977) recognized different morphological structures associated with travertine deposition at Fall Creek, Idaho. He noted that the local topography, biologic activity, seasonal climatic change, and flow rate all contribute to the character of the spring deposit formed.

CHAPTER II

METHODOLOGY

Sampling

The freshwater carbonates were sampled in the field so as to best represent different megascopic textures and subtle lithologic variations. The number of samples collected from each locality varied depending on the aforementioned factors and the availability of fresh outcrop material. In one instance, 11 samples were taken from a core (e.g., CB-2 to CB-12).

Due to the nature of their occurrence, the various carbonate deposits were not mapped geologically. However, a thorough reconnaissance of the outcrop areas was carried out and an attempt was made to note the topographic profile and megascopic structures present. Thirteen samples were selected for petrographic study.

Chemical Analysis

After separating weathered from relatively fresh material, samples were crushed in a ceramic jaw crusher and then pulverized in a Spex ball mill using tungsten carbide balls and chamber. Ground samples were then sieved to -80 mesh or finer.

Atomic Absorption

Calcium, magnesium, iron, manganese, strontium, sodium, potassium, lithium, barium, zinc, lead, copper, chromium, and nickel were determined with a Perkin-Elmer 403 double-beam atomic absorption spectrophotometer using instrument settings recommended by the manufacturer. Samples to be analyzed by atomic absorption were prepared by dissolving 1 gm of rock powder in a solution of 40 ml of 10% hydrochloric acid. After digesting for approximately 18 hours in a teflon beaker at room temperature, samples were heated at 65° C on an electric hot plate for an additional 6 hours. The solution was then filtered in order to separate-out all insoluble residue. Any residue fraction was dried and weighed for use in determining bulk rock chemistry. To insure accurate determination of barium and strontium, one per cent lanthanum solution was added and each aliquot was brought to 50 ml volume with deionized water.

The atomic absorption spetrophotometer was calibrated using standards prepared from 1000 ppm atomic absorption grade stock. Standard concentrations were chosen according to known elemental compositions in similar carbonate rocks.

Eighty-eight carbonate samples were analyzed for the elements listed. Analyses were reconverted to soluble fraction by dividing elemental concentration by one-minus insoluble residue.

Factor analysis between the various elements was performed using a Statistical Analysis System packaged program.

X-ray Diffraction

X-ray analysis was used to determine the carbonate mineralogy of some samples and to confirm the complete dissolution of any carbonate fraction in the insoluble residue. A Philips Model 12645 diffractometer using CuKα radiation and nickel filter was utilized for this purpose. The X-ray tube was operated at a potential of 35,000 volts and a current of 20 milliamps. Signal was detected using a flow proportional counter.

A slow scan speed (1/8° per min), coupled with a high reolution collimator and slits, enabled differentiation of peak shift between 26° and 31.5° two-theta. An internal standard of CaF_2 was mixed with each sample for calibration and special mounting blanks were used to attain a constant volume percent. Mole percent magnesium was determined using the graph by Scholle (1978). Thirty representative samples were chosen for this analysis by random number methods.

In addition, some insoluble residues were qualitatively scanned (2° per min) between 2° and 100° two-theta for purposes of identifying major mineral constituents. Furthermore, several specimens were X-rayed based on unusual elemental compositions determined by atomic absorption analysis. In one instance, spot X-ray analysis of a thin section confirmed mineral recognition suggested by petrographic studies.

CHAPTER III

DESCRIPTION AND GENERAL GEOLOGIC SETTING

Four main deposits have been studied in detail and separate discussion is devoted to each. Three of these locations are in Colorado and were investigated personally by the author. The fourth deposit, in New Mexico, was sampled and described by Dr. R. Nowell Donovan. The remainder of the samples used for analysis were collected from a variety of sources in the United States and the United Kingdom.

Twin Mountains

The region of Twin Mountains is located approximately 6.5 km northwest of Cañon City, Colorado along the north side of State Highway 50. The area is complex structurally, consisting of a series of plunging folds offset by numerous reverse faults of post-Pennsylvanian age. The rock units present range from Precambrian granite to Pennsylvanian arkose.

Lying along the unconformable geologic contact between the Fremont Dolomite (Ordovician) and the Fountain Formation (Pennsylvanian, composed of poorly sorted arkosic sandstone and conglomerate) is a large travertine deposit. This deposit is situated along the flank of a broad valley. The trend of the long axis of the travertine deposit is 120° and it is approximately 275 m long. Two poorly developed joint sets cut the deposit at 050° and 100°. The travertine probably is

Pleistocene, but the exact time of formation is not known.

The travertine has been quarried extensively since the early 1900's, but the general geometry and configuration of the deposit still is readily apparent. The travertine appears as a series of 5 terrace-like mounds which progress downward toward the floor of the valley (Figs. 1 and 2). The individual terraces are generally from 9 to 10 m thick, 15 to 20 m wide, and 45 to 60 m in length.

The terrace-like development of the travertine appears to be characteristic of carbonates precipitated from freshwater running downslope. Many contemporary travertine deposits exhibit this same feature (Fig. 3). As water seeps on to the sloping hillside, $CO_2^{=}$ from the $Ca(HCO_3)_2$-rich solution is lost to the atmosphere and $CaCO_3$ is deposited with an initial dip equal to the slope upon which it is being deposited. Irregularities or obstructions on the slope help form small travertine "dams" and lead to the development of shallow ponds. This process causes the formation of an upward growing series of terraces as long as the slope, flow rate, and water composition remains in equilibrium with the environment of deposition.

Once a terrace pool has developed, continued precipitation causes the depositional dip to decrease until bedding is horizontal. At any given time, overflow from the pool on its downslope margin will "feed" a lower-level prograding terrace. Fig. 4 illustrates the process of terrace development.

Field evidence strongly supports the depositional model in Fig. 4. The travertine terraces are generally horizontally bedded, with the exception of the northwest margin of the uppermost terrace where depositional dips up to 15° are present. In this latter area, the

Fig. 1.-Twin Mountains. Elevated view of travertine quarry looking toward the southwest. Note at least three distinct terrace levels of travertine are discernible.

Fig. 2.-Twin Mountains. Same view as Fig. 1, but this photograph was shot looking toward the northeast from below the second terrace. Note distinct horizontal bedding in the deposit.

Fig. 3.-Opal Terrace, Mammoth Hot Springs, Yellowstone National Park. Note the characteristic terrace-like appearance of the travertine deposits.

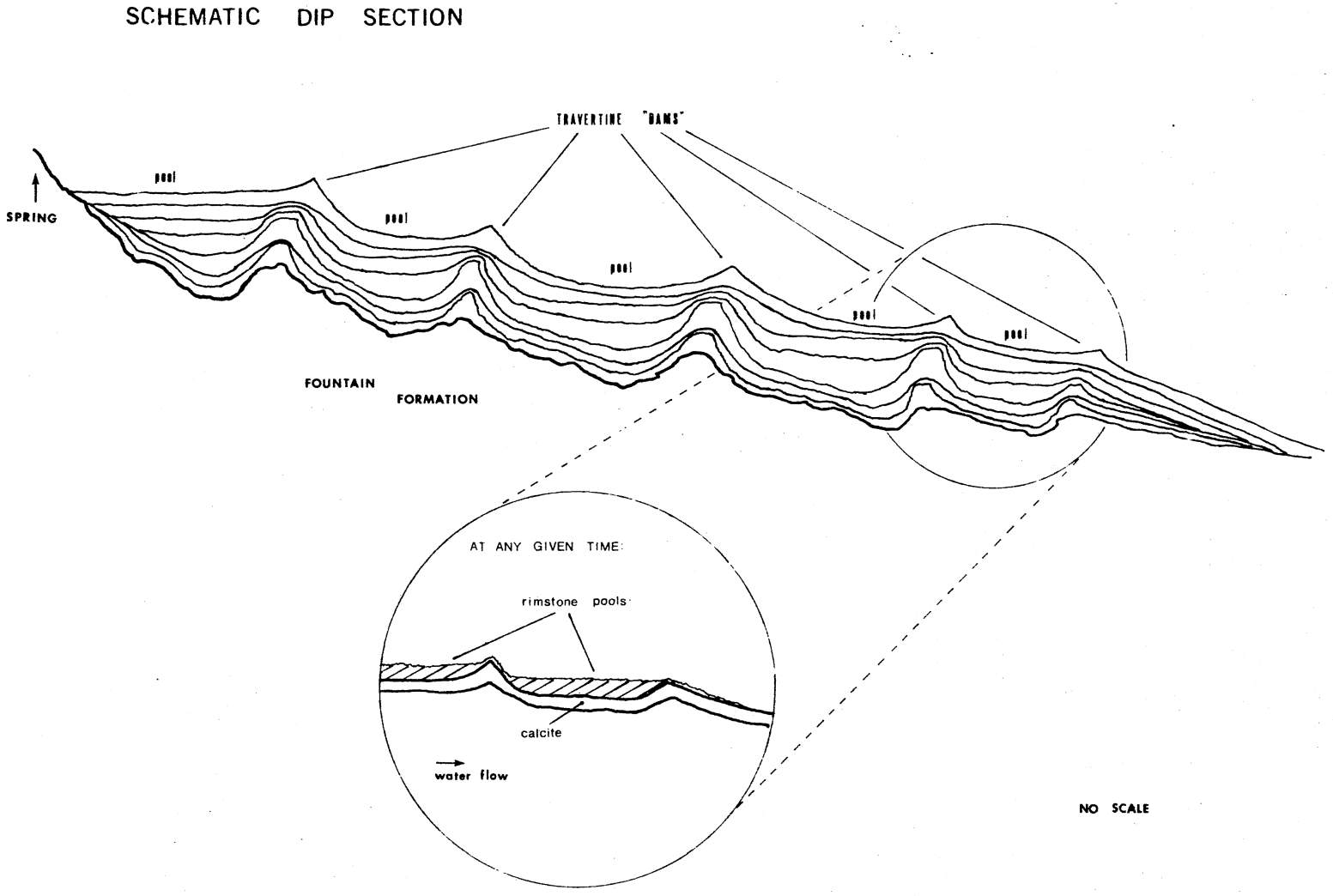

Fig. 4.-Twin Mountains. Field sketch illustrating cross-sectional appearance of the Twin Mountains travertine deposit. Inset displays the mode of formation at any given time during the terrace history.

thickness of travertine is only about 1 m and no evidence of terrace formation is seen.

Disrupted bedding structures are readily visible in some areas (Figs. 5, 6, and 7). These features may record penecontemporaneous disruption and slumping of partially consolidated travertine, conceivably as a result of earthquake shock. Although similar structures are attributed to stromatolitic-type development in many areas (Herlinger, 1977), field observations failed to uncover any evidence of biogenic influence.

The spring that deposited the travertine is now dry. A possible conduit located within the uppermost terrace indicates that water movement may have been related to a large fault which crosses the top of the quarry area. On the basis of field evidence, the deposit is considered to be the product of hydrothermal activity. Evidence does not indicate multiple spring centers.

Guffy

Located approximately 12.8 km west of Guffy, Colorado and 32 km east of State Highway 9, is a small mound of recent travertine currently being enlarged on top of Precambrian granite (Fig. 8). This material is being precipitated by two springs located along the strike of the valley. Both springs appear to be decreasing in activity. The time span of the deposit is unknown, but a small well house located on top of the mound deposited by the larger spring was constructed in 1954. Because only the larger spring has developed any appreciable travertine accumulation, detailed analysis is restricted to this area.

Fig. 5.-Twin Mountains. Contact between Fountain Formation (F) and travertine (T). Note the disrupted and contorted bedding within the basal section of the travertine.

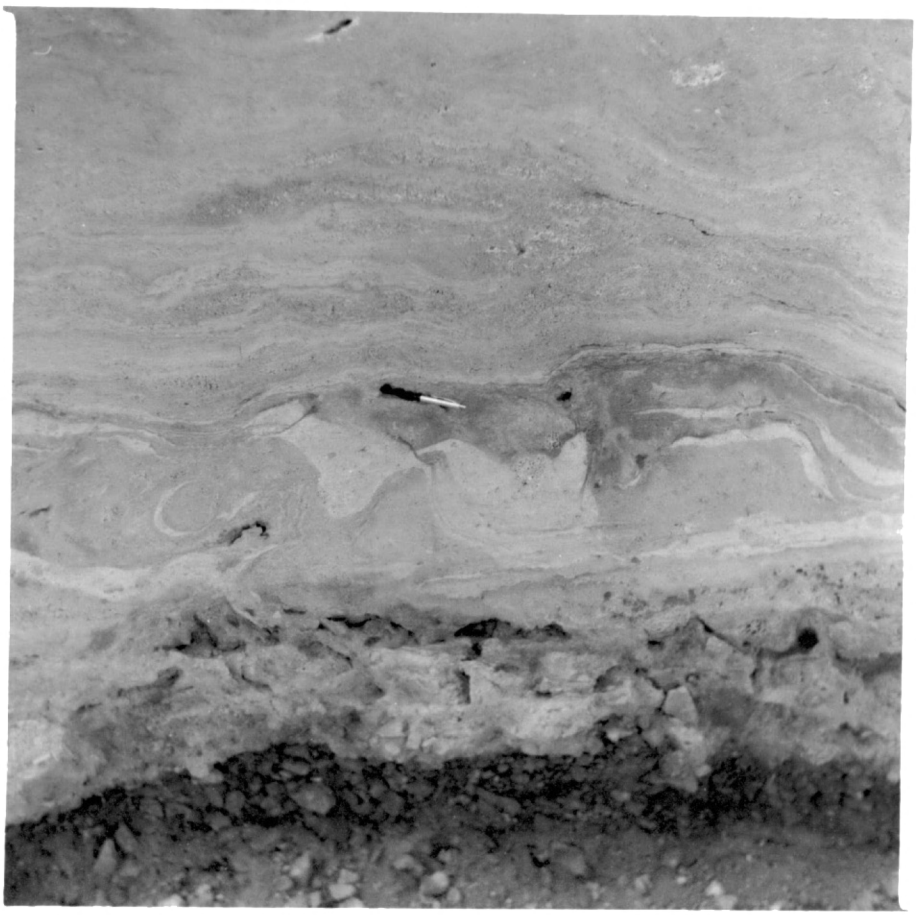

Fig. 6.-Twin Mountains. Disrupted bedding in travertine. Same as Fig. 5, but field of view reduced to show detail.

Fig. 7.-Twin Mountains. Close-up view of contorted bedding within travertine. This photograph was shot approximately 2 m above the travertine-Fountain Formation contact.

Fig. 8.-Guffy. Mound of recent travertine, about 4 m high, formed on top of Precambrian granite. Wooden structure partially surrounds dying spring. Water temperature is about 12° C.

Fig. 9.-Guffy. Spring well on top of travertine mound. Note the emerging bubbles and the bright orange bottom material.

Fig. 10.-Guffy. Surface of travertine mound showing the intricate terracette development. Broader terracettes are associated with more gentle slopes (see Fig. 11).

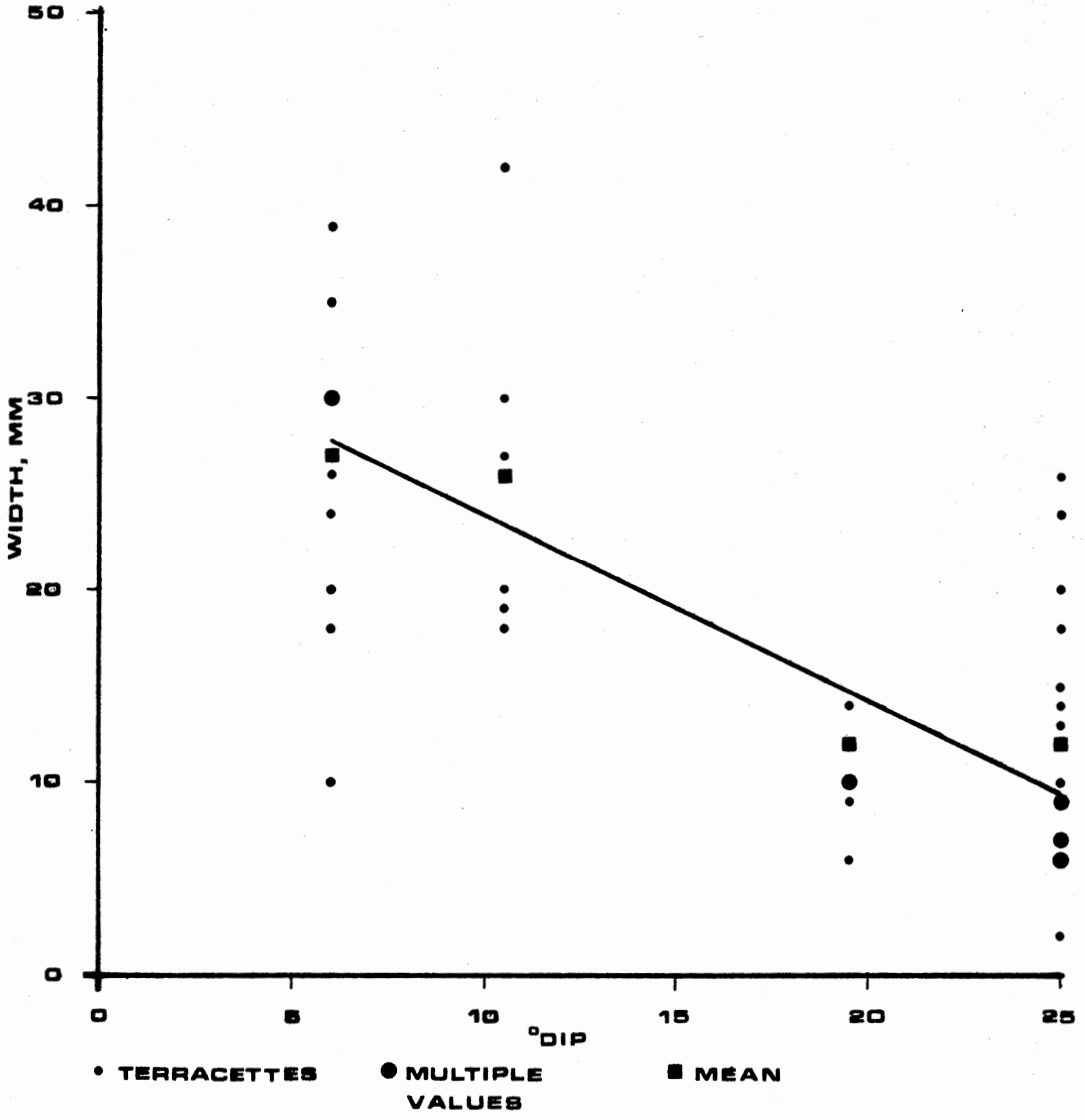

Fig. 11.-Guffy. Plot of width (mm) versus degrees-dip for individual terracette surfaces. The four populations represent natural groupings of 38 field measurements.

Volumetric calculations based on conical dimensions show that approximately 65 m^3 of travertine has been deposited in this area. More precise calculations based on erosional or depositional cycles are impossible without additional data.

Kelly Ranch

The study area is situated approximately 5 km northwest of the junction of Colorado State Highways 50 and 115. A series of travertine mounds is located along the unconformable Dakota Sandstone (L. Cretaceous) and Graneros Shale (U. Cretaceous) geologic contact. These deposits trend 140° and cover an area 450 m wide by 270 m long. Eight ellipsoidal mounds are recognizable with heights ranging from 4 to 6 m (Fig. 12). Bedding is highly irregular with depositional dips up to 17°. In some areas, 2 to 3 definite generations of carbonate deposition are visible. Field observations suggest at least two mounds might contain some iron-rich carbonate, as evidenced by a yellowish goethite-stained surface.

The springs that precipitated these deposits are now extinct, but apparently they emerged through a prominent 145° joint set developed in the Dakota Sandstone hogback. This joint set strongly controls local erosion and travertine deposition postdates local erosional patterns.

The age of these deposits is unknown, but an early Cañon City quadrangle map (1880) shows permanent streams flowing in this general vicinity. Local residents recall "soda springs" that died out in the early 1900's subsequent to the drilling of artesian wells near Florence, a town approximately 8 km due south of the study area

Fig. 12.-Kelly Ranch. Small ellipsoidal travertine mound, about 5 m high. Pisolites are present near the top of the deposit.

(Alex Ross, personal communication). If "cold" water springs were present, groundwater deposition would be responsible for the travertine accumulation.

However, hydrothermal deposition might more plausibly account for the carbonate build-ups. Where the mounds rest on flat-lying terrain, they have an appearance suggestive of forceful ("geyser-like"?) egression. Furthermore, the obvious tectonic control of depocenters might favor a hydrothermal interpretation. Unfortunately, no data are available on the water temperature or chemistry of the old springs.

Soda Dam

Soda Dam is located approximately 60 km due north of Albuquerque, New Mexico at the junction of State Highway 4 and the Jemez River. The geology of the area is dominated by the Valles Caldera volcanic complex 5 km northeast of the study area. Rocks exposed include Precambrian granite, Paleozoic and Mesozoic sediments, and Tertiary and Quaternary volcanics and alluvial fill. Water discharged by thermal and cold mineral springs is believed to be derived in part from a hydrothermal reservoir in Valles Caldera and to flow out along a ring-fracture zone, largely in limestone that overlies the granitic rock. Soda Dam is a travertine accumulation associated with these emerging springs.

The major travertine deposition is localized along a prominent northeast-southwest trending normal fault which brings an isolated mass of Precambrian granite up against Pennsylvanian limestone of the Magdelena Group (Fig. 13). Several smaller travertine accumulations are also present along adjacent subsidiary faults (Fig. 14).

Fig. 13.-Soda Dam. View northwest along main travertine mass. Extinct feeding conduits were located along the top of the mass in a line marking the controlling fault. Late veins, parallel to this trend, which cut the travertine, contain calcsparite and a little galena.

Fig. 14.-Soda Dam. Isolated mound of travertine, about 10 m high, fed by an extinct conduit controlled by a minor north-south trending fault. High initial dips are conspicuous, particularly toward the exterior of the mound.

In 1902 there were 22 springs flowing along the dam; by 1912 only 11 springs; now only 5 are still flowing (Kelley et al., 1961; Figs. 15 and 16). High on the west wall of the canyon, 280 m above the present river level, are remains of older "dams" formed before Jemez River had cut to the present level.

The temperature of the water in the five springs varies from 34° C to 47° C; collectively this water raises the temperature of the Jemez River by about 1.5° C. Field sampling of the five springs showed pH readings between 6.1 and 7.4.

Large terraces of travertine are not well-developed in the deposit and initial dips increase away from individual spring orifices (Figs. 13, 14, 17, 18 and 20). Two of the springs are characterized by the terracette features previously described in the Guffy deposit (Figs. 15 and 19).

The travertine deposit has incorporated regolith along its base and, where it has bridged the Jemez River, tree debris from the river is coated by carbonate.

A late feature, cutting the main travertine mass, is a number of subvertical veins, parallel to the main controlling fault and infilled by coarse sparite and a little galena (Fig. 13). It is clear that fault movement has occurred since most of the travertine formed, for in addition to the veins, a fault scarp is present at the southeast end of the main mass (Fig. 18). This scarp shows a slight amount of vertical slickensides.

Soda Dam was the site of the first discovery of pisolites and oölites in a spring deposit in North America (Kelley et al., 1961). During the present study, oölites were found in the orifices of two

Fig. 15.-Soda Dam. Active spring overlain by main mass of travertine. Terracettes are conspicuous (see Figs. 19 and 20). Water temperature is about 34° C.

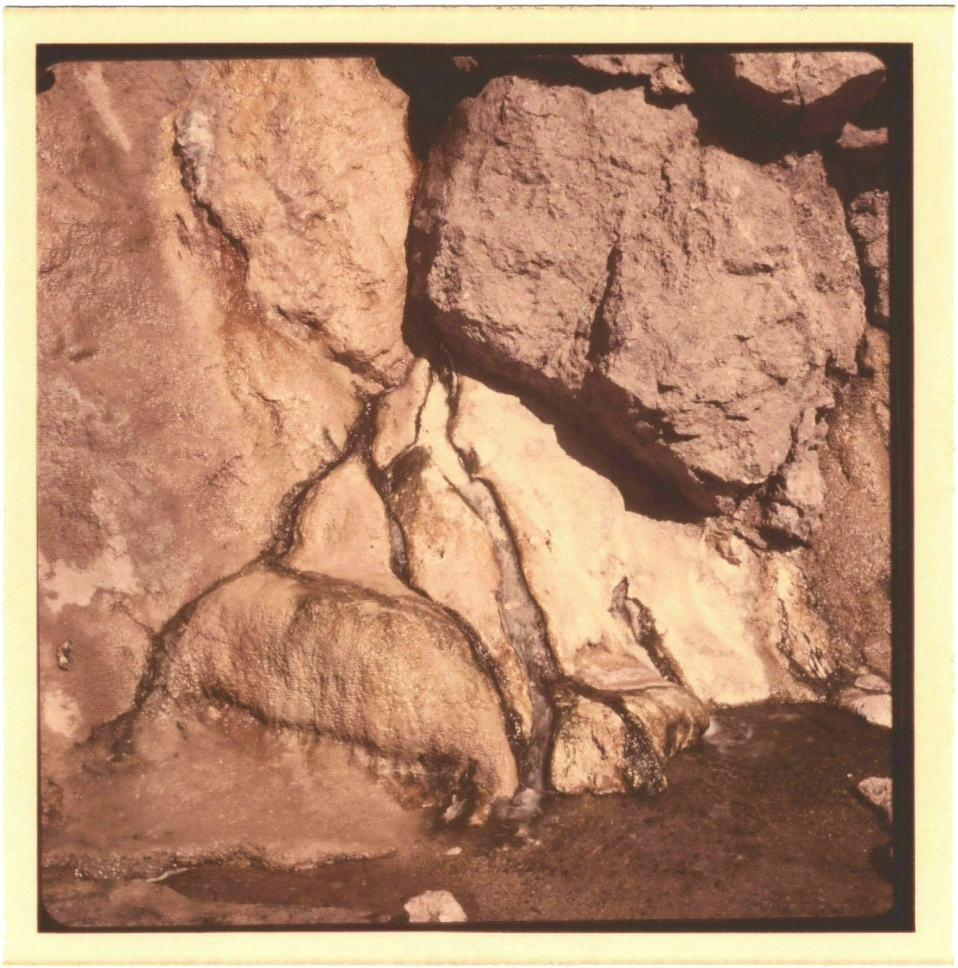

Fig. 16.-Soda Dam. Roadside spring. The water has a temperature of about 47° C. Note the algal growth.

Fig. 17.-Soda Dam. Two extinct springs immediately north of the main travertine mass (the smaller of the two is adjacent to the hammer). Oölites and pisolites occur in both orifices.

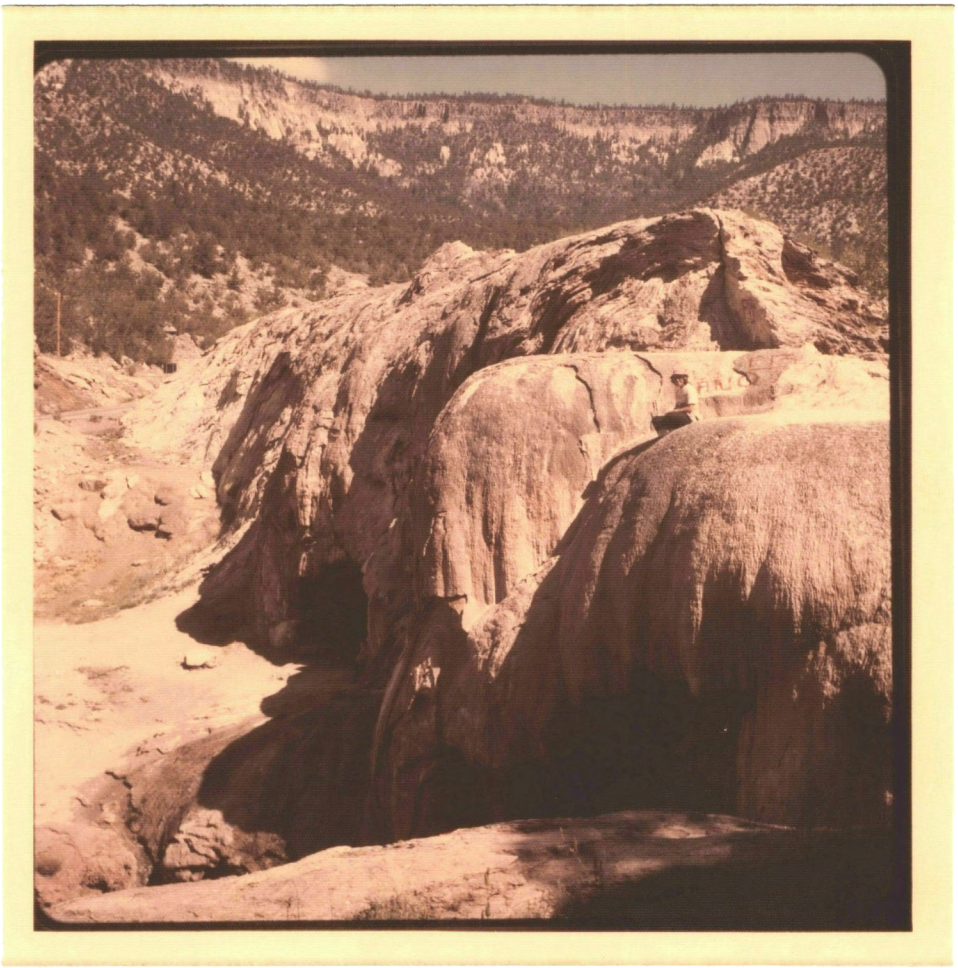

Fig. 18.-Soda Dam. View northwest along the main travertine mass. Note the high initial dips of travertine. Immediately above and to the right of the figure the trace of the controlling fault is visible as a small scarp.

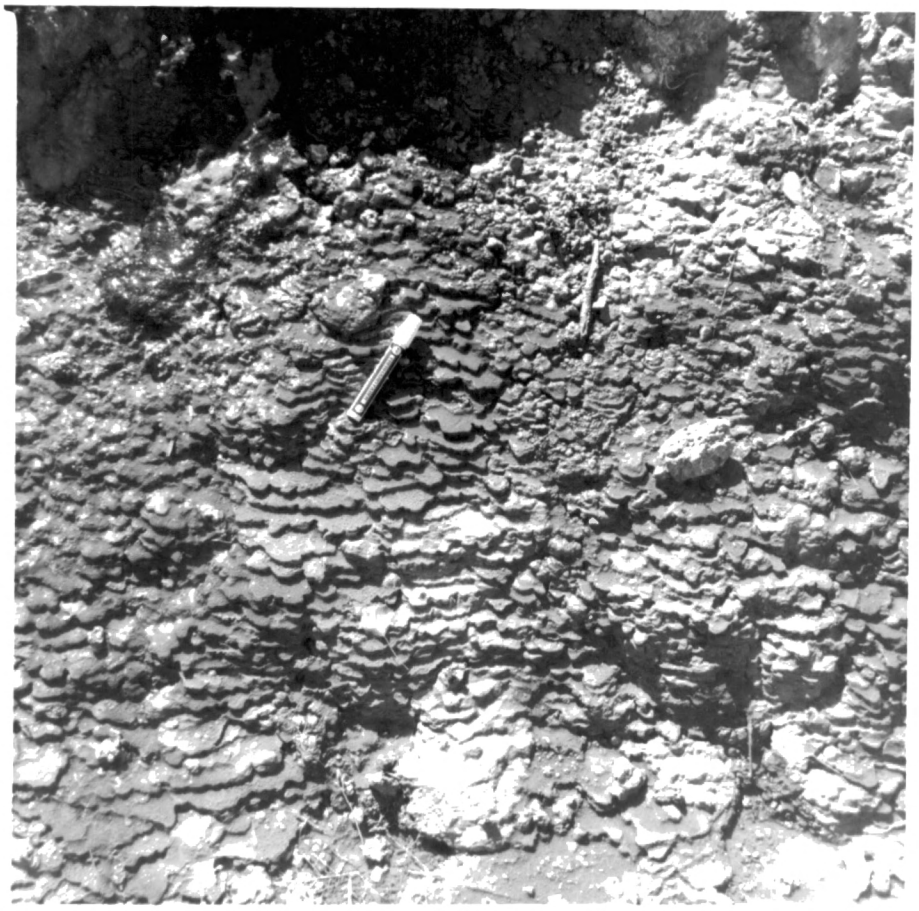

Fig. 19.-Soda Dam. Terracette structures developed close to an active spring. The wider terracettes are clearly associated with more gentle slopes.

Fig. 20.-Soda Dam. The main travertine mass has bridged the Jemez River. Most springs in the mass are extinct. The one depicted in Fig. 15 is located in the cave immediately above the two figures.

extinct springs immediately north of the main travertine mass (Fig. 17). It is probable that these formed as the result of agitation of detritus in a carbonate-saturated pool immediately prior to the extinction of the spring. This theory of formation is broadly analogous with that involving the formation of cave pearls.

CHAPTER IV

LITHOLOGY AND PETROGRAPHY

Hand Specimen Appearance

Characteristically, all the travertine accumulations appear as mound or terrace-like masses which have formed as the result of precipitation from carbonate-saturated spring waters. Surfaces commonly are irregular and very porous, consisting of a micritic carbonate groundmass. Abundant cavities commonly contain secondary carbonate vug filling and, rarely, clay.

Local detrital fragments of bedrock and vegetation, trapped during the initial carbonate deposition, are generally found within the lower portions of the travertine masses (Fig. 21). In these lower areas, depositional dips may be seen, usually in juxtaposition to spring orifices.

In some travertines, distinct carbonate laminae are recognizable; this feature is more sharply defined microscopically than megascopically. Rarely, remnant oölites and pisolites are present in association with extinct spring pools (Fig. 22; see Fig. 17).

Mineralogy and Texture

Twelve specimens from the Twin Mountains and Soda Dam localities were examined using a petrographic microscope with a plane-polarized

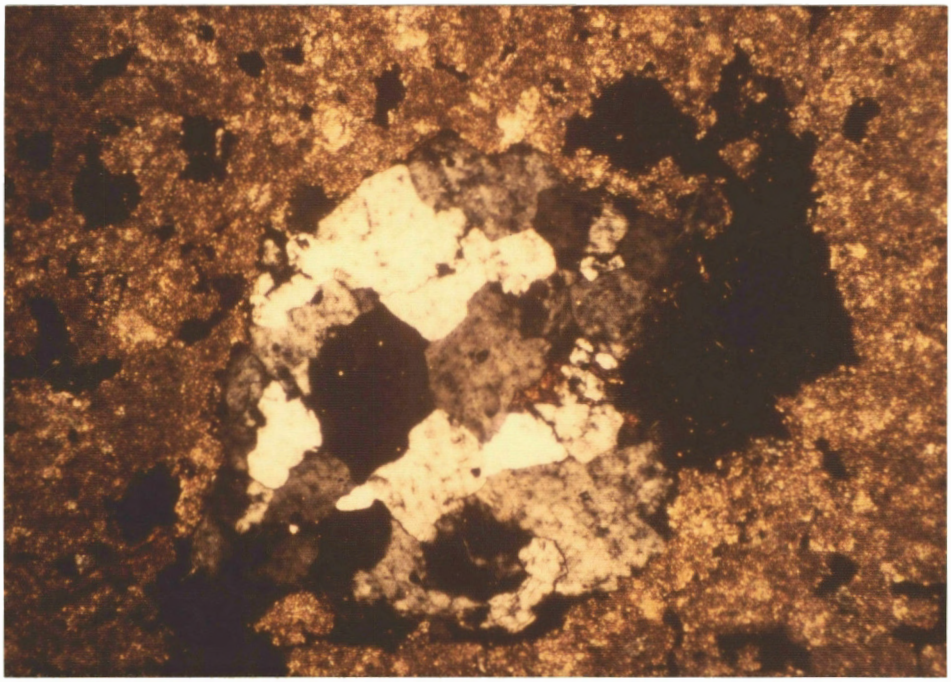

Fig. 21.-QII288. Rock fragment within primary micrite fabric. The fragment was probably derived from the underlying arkosic conglomerate of the Fountain Formation. Field of view 1.66 x 2.40 mm, crossed nicols.

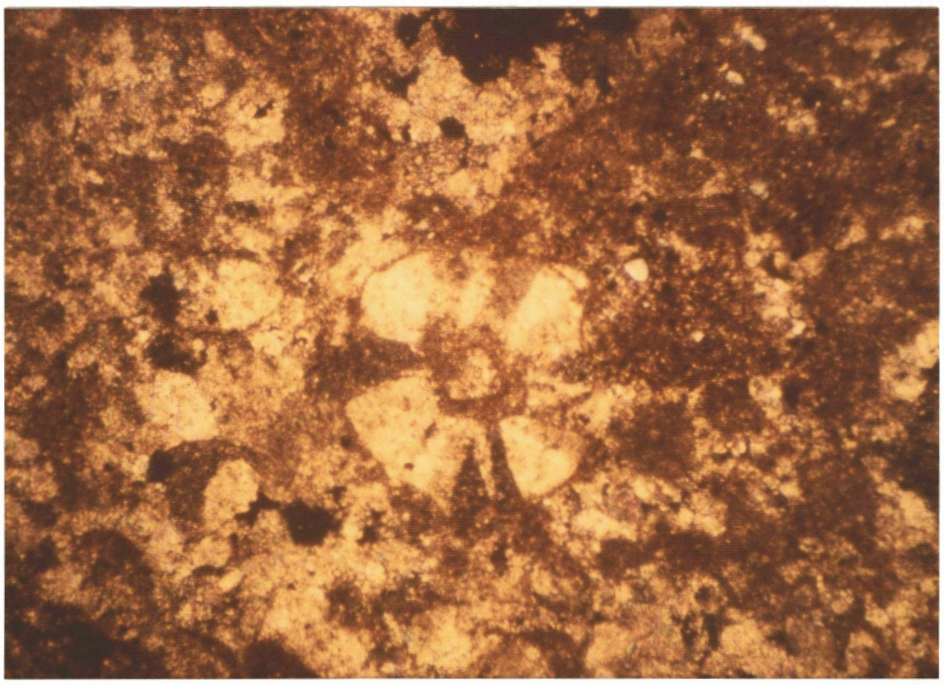

Fig. 22.-QIB. Concentric oölitic structure within microsparite fabric. It appears that a calcite fragment became coated with terrigenous clay, acting as a nucleus for subsequent radiaxial growth of fibrous calcite. Rotation of the microscope stage shows undulatory extinction throughout the fibrous crystals. Field of view 1.66 x 2.40 mm, crossed nicols.

light source. One thin-section from the Verde Formation, a lake carbonate of Pliocene age, was analyzed for comparison. In addition, a limited amount of petrographic study was conducted using cathodo-luminescence methods. Scanning electron microscopy was used to study special textures from all localities.

Thin-section analysis reveals that the dominant texture is a mozaic of anhedral equigranular micrite which forms an irregular spongy texture. This porous texture is variably and partially infilled by microsparite (Figs. 23 and 24; Appendix A). Overall, very little coarse sparry calcite is developed, and it is usually restricted to the interiors of cavities (Figs. 25 and 26). The number of precipitation episodes is generally difficult to determine under the optical microscope due to the absence of recognizable laminations. However, cathodo-luminescence study suggests that usually more than two depositional events have occurred (Fig. 27). Where present, lamination is erratic and is not related to stratigraphic position within the section. No organic textures appear in any of the sections and the carbonate precipitation is interpreted to be strictly abiogenic.

Clay minerals are present as widely scattered terrigenous flakes. Illite and kaolinite are the dominant clay species with kaolinite being the most abundant. Chlorite is present in some sections, but always in trace amounts.

Porosity is generally high; values from 3-42% with a mean porosity of 20.5% were recorded. There appears to be no correlation of percentage porosity with location in the deposit. In general, the finer-grained the matrix, the lower the porosity value.

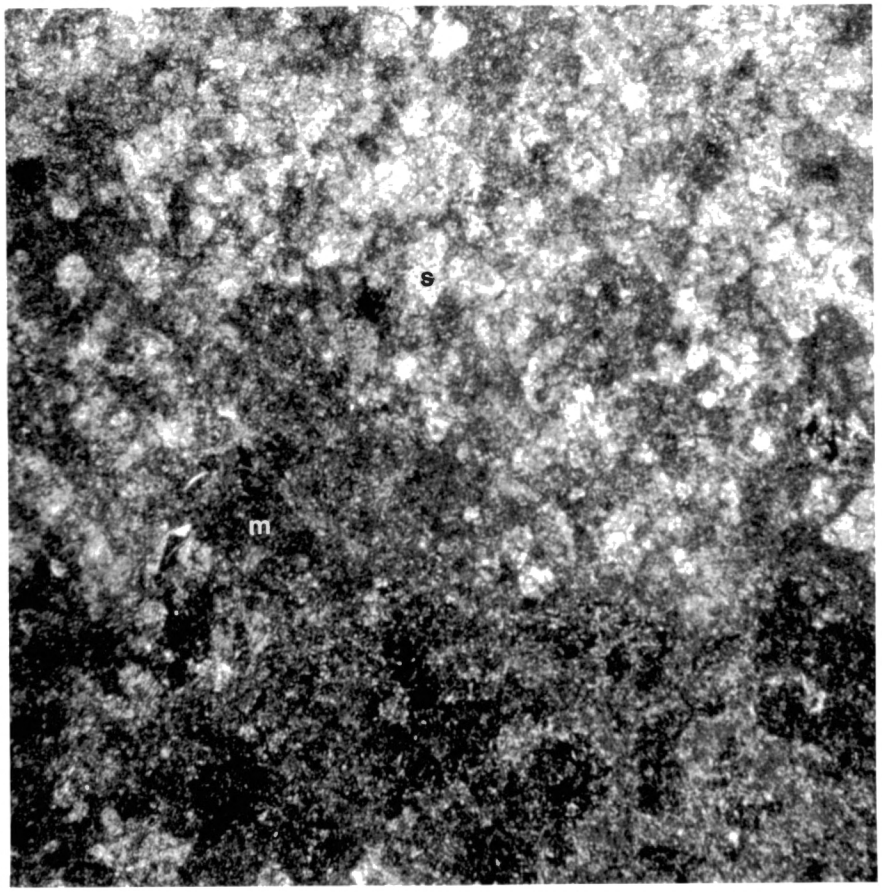

Fig. 23.-M1. Typical fabric of micrite (m) and microsparite (s) forming a rigid carbonate framework. Field of view 1.66 x 2.40 mm, crossed nicols.

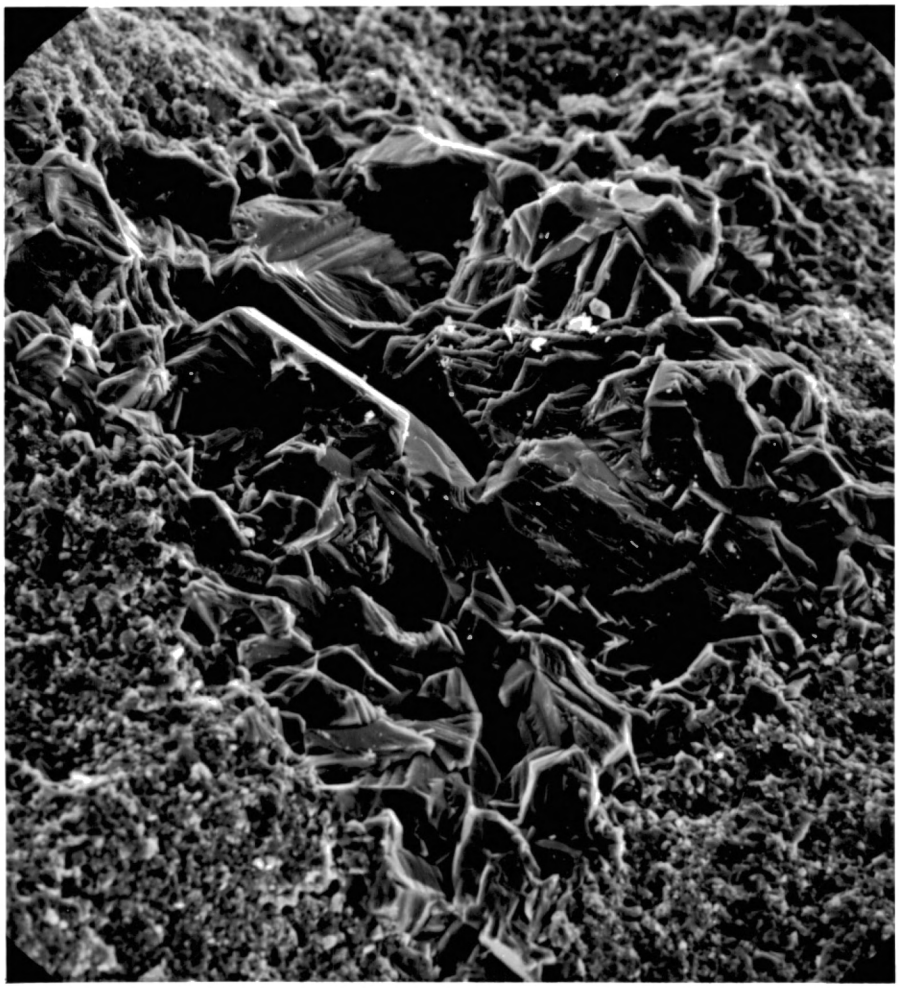

Fig. 24.-QSPTA. Scanning electron micrograph showing a cavity infill by sparite. The primary fabric is anhedral equigranular micrite. The sparite shows drusy growth and some euhedral faces in the center of the cavity, (x200).

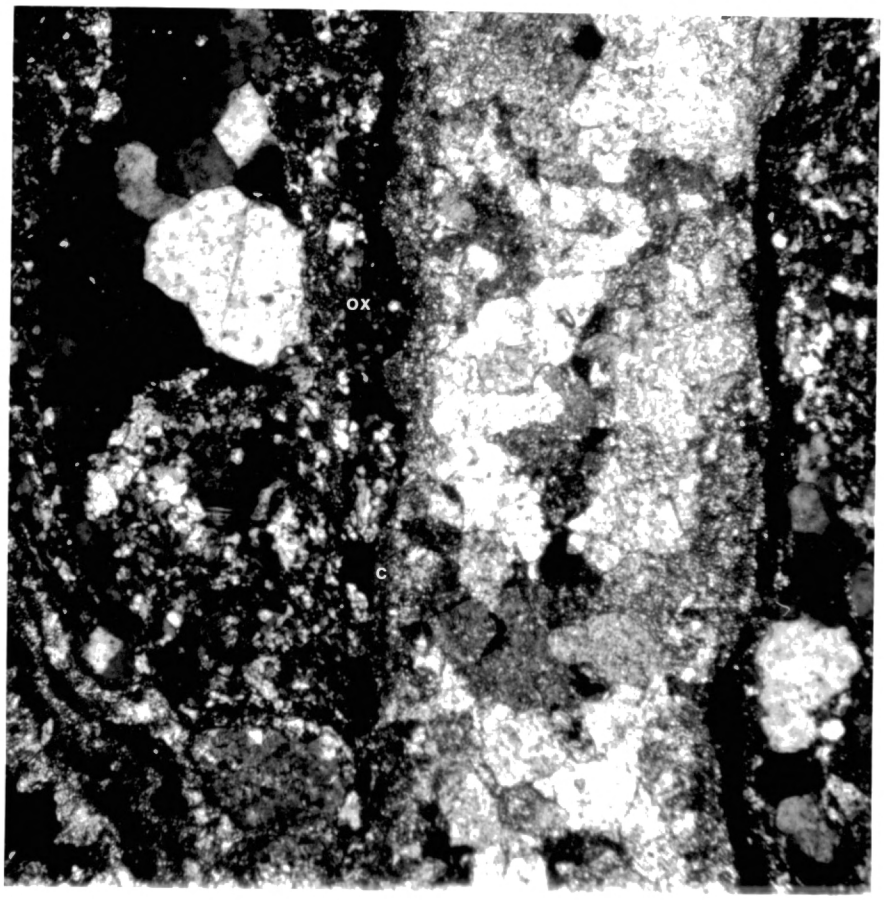

Fig. 25.-SPII. Vein infill by sparite (euhedral toward the void). Iron oxides (ox) and clay (c) separate the later pore infill from the primary carbonate fabric. Field of view 0.45 x 0.63 mm, crossed nicols.

Fig. 26.-GI45FS. Scanning electron micrograph showing cavity with well-developed sparite crystals. Note the distinct rhombohedral cleavage in large crystal, (x78).

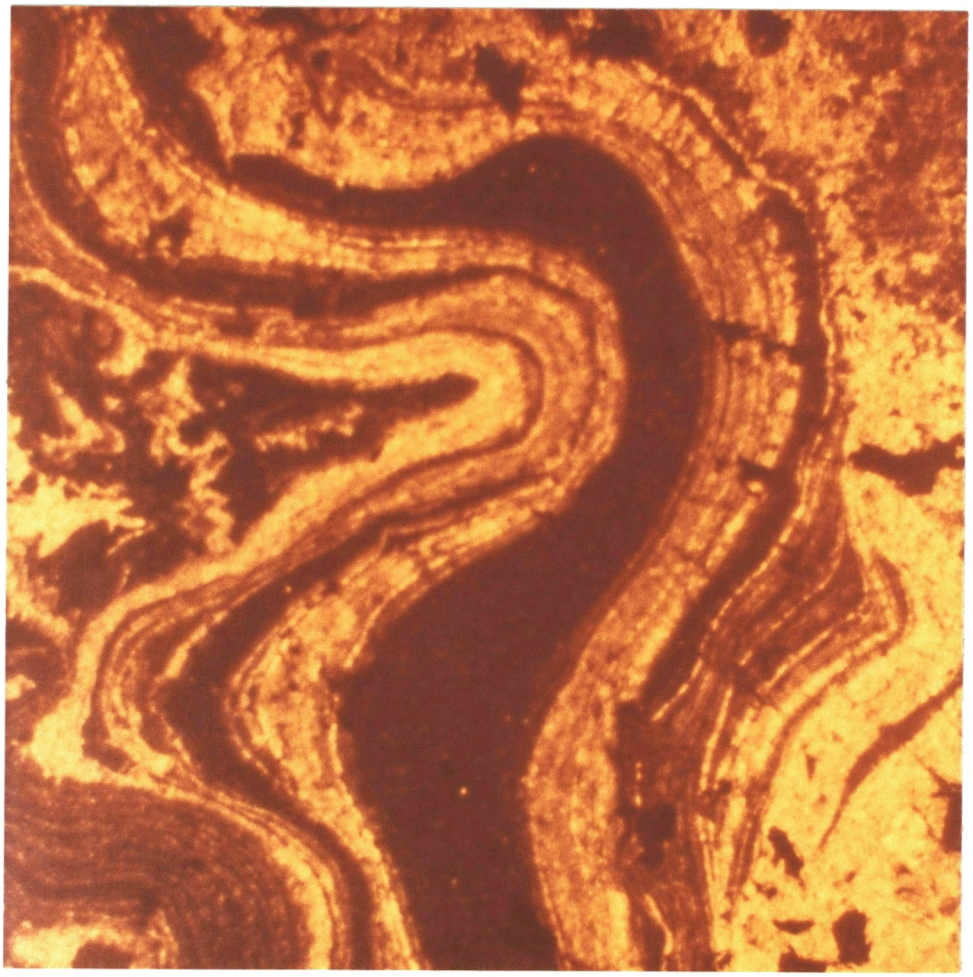

Fig. 27.-B. Cathodo-luminescence photomicrograph showing multiple stages of accretionary carbonate precipitation. The contrasting intensities and shades of orange are a function of differences in the iron content of the carbonate lamina. Field of view 1.66 x 2.40 mm.

In several samples, the following diagenetic sequence can be constructed:

1) Primary fabric deposition of micrite and microsparite formed a rigid carbonate matrix.
2) Incorporation of detrital clay (rare) and iron oxide precipitation (common) developed as pore linings.
3) Pores were filled by secondary carbonate.
4) Ocasionally, veining and coarse drusy sparite infill are present. The luminoscope shows growth by episodic accretion involving fluctuations in the iron content (Fig. 25).
5) At Soda Dam, precipitation of lead sulfide followed vein infill.

Pore filling carbonate did not assume the same crystal form. Calcite is commonly present as both fibrous and equant-grained spar (Figs. 28, 29, 30, and 31). In two specimens, abundant acicular aragonite and high-Mg calcite crystals dominate as the void cement (Figs. 32, 33, 34, and 35). A similar arrangement of low-Mg calcite crystals, termed "whisker cement," has been described by Scholle (1978) as a vadose-zone phenomenon in Pleistocene limestone from Florida.

X-Ray Diffraction

X-ray diffraction studies of thirty selected freshwater carbonates showed that all samples were contained within a range of 4-30 Mol % Mg (Appendix B), when applied to a plot of 2θ (degrees) versus Mol % Mg (Scholle, 1978). Using this criterion for classification, the samples were identified as either high-Mg or low-Mg calcite (Fig. 36).

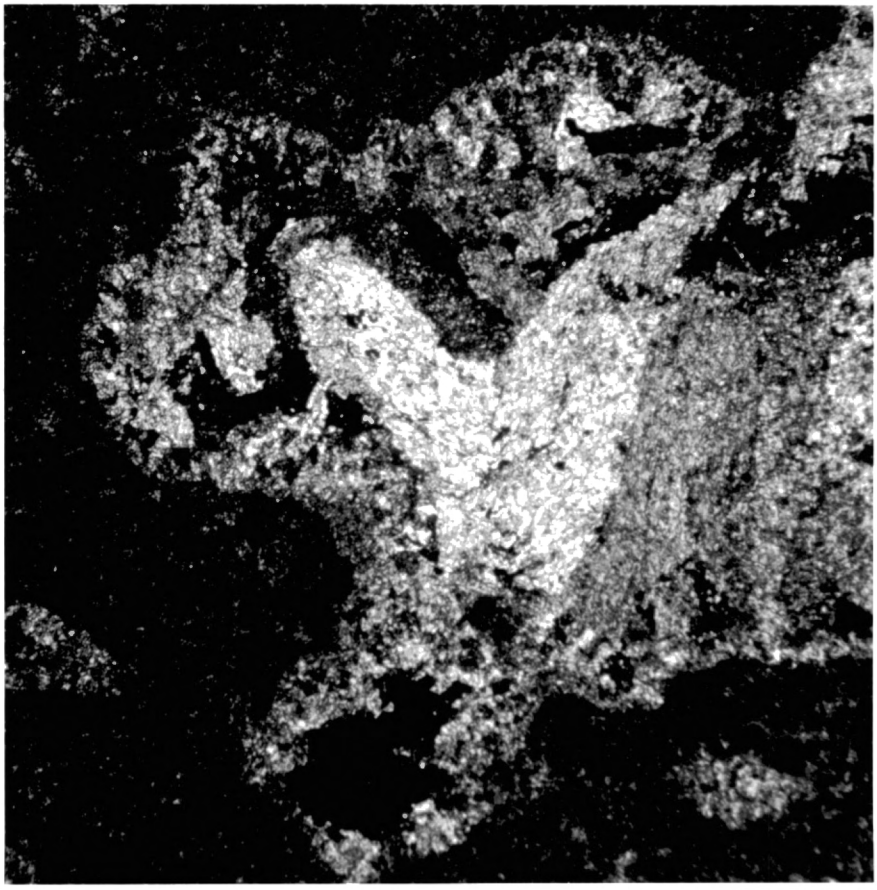

Fig. 28.-QII150. Fibrous calcite crystals partially filling void space. Field of view 1.66 x 2.40 mm, crossed nicols.

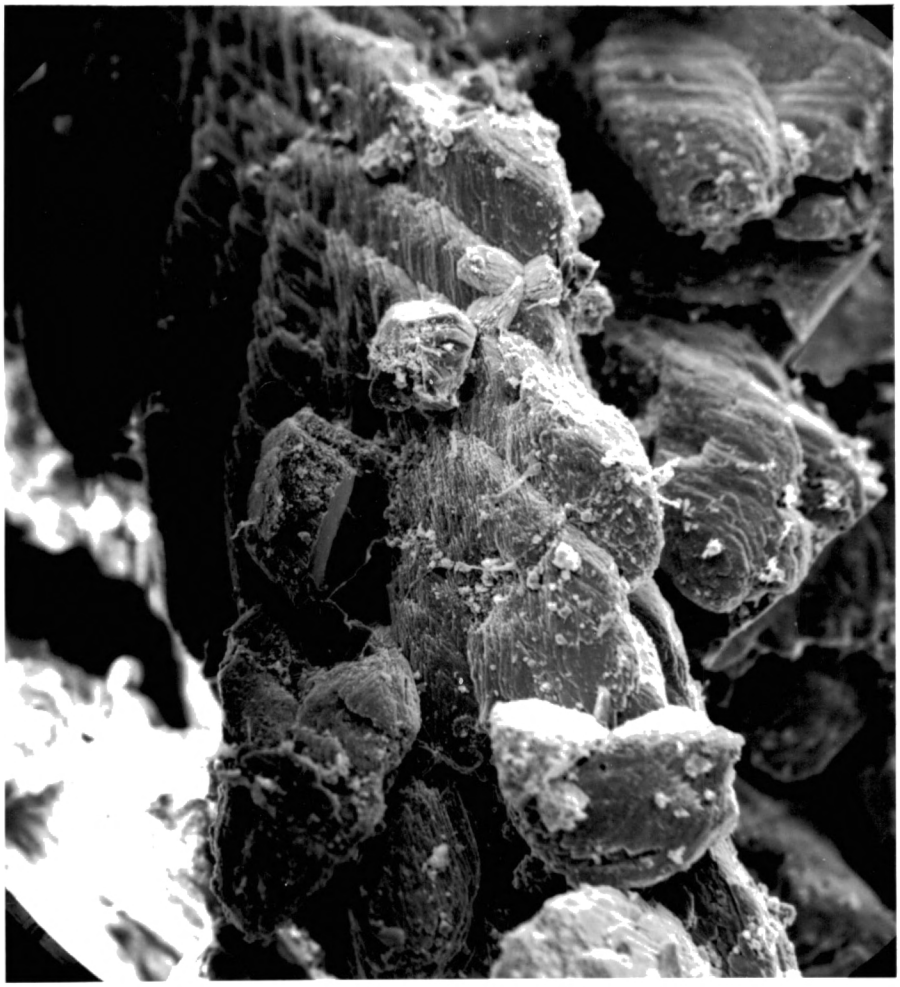

Fig. 29.-GUFIB. Fibrous crystals are seen to be "rod"-shaped aggregates of calcite with continual offset of crystal axes along a preferred orientation. Smaller calcite rhombs grow on the "rod", (x110).

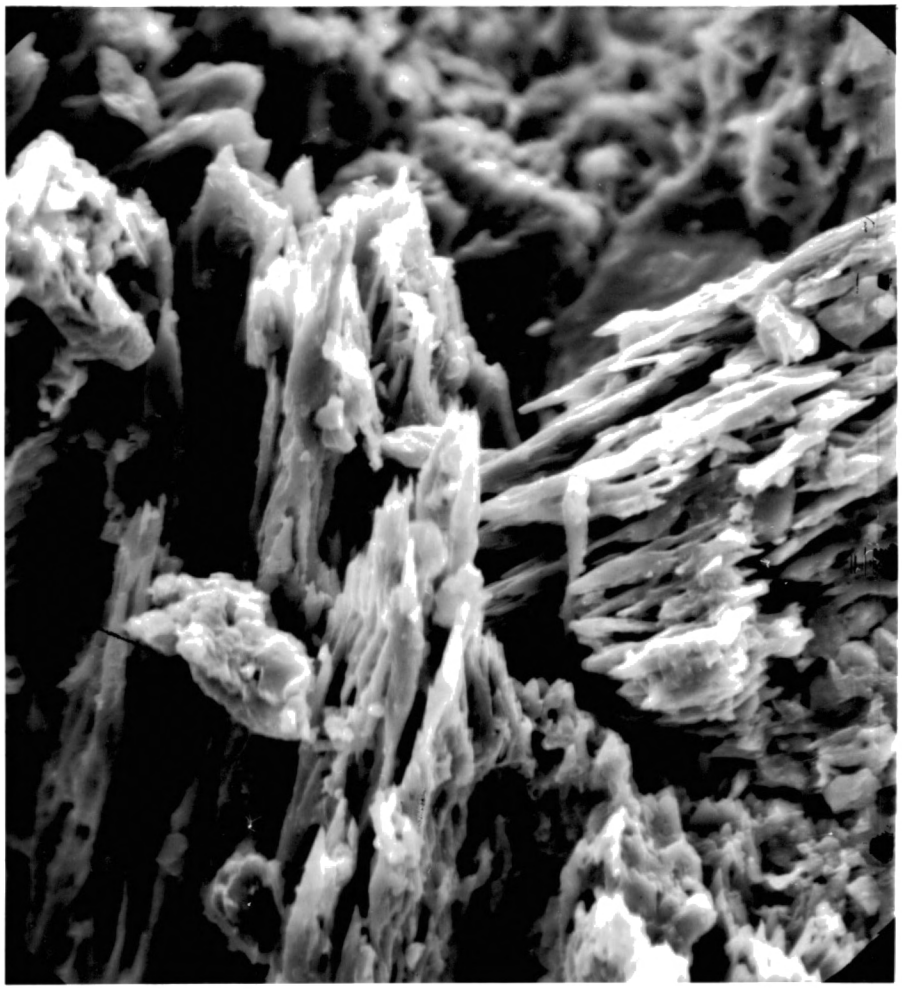

Fig. 30.-B. Scanning electron micrograph of fibrous calcite crystals filling a void at Soda Dam. Although superficially resembling aragonite, crystallographic detail attests to calcite, (x780).

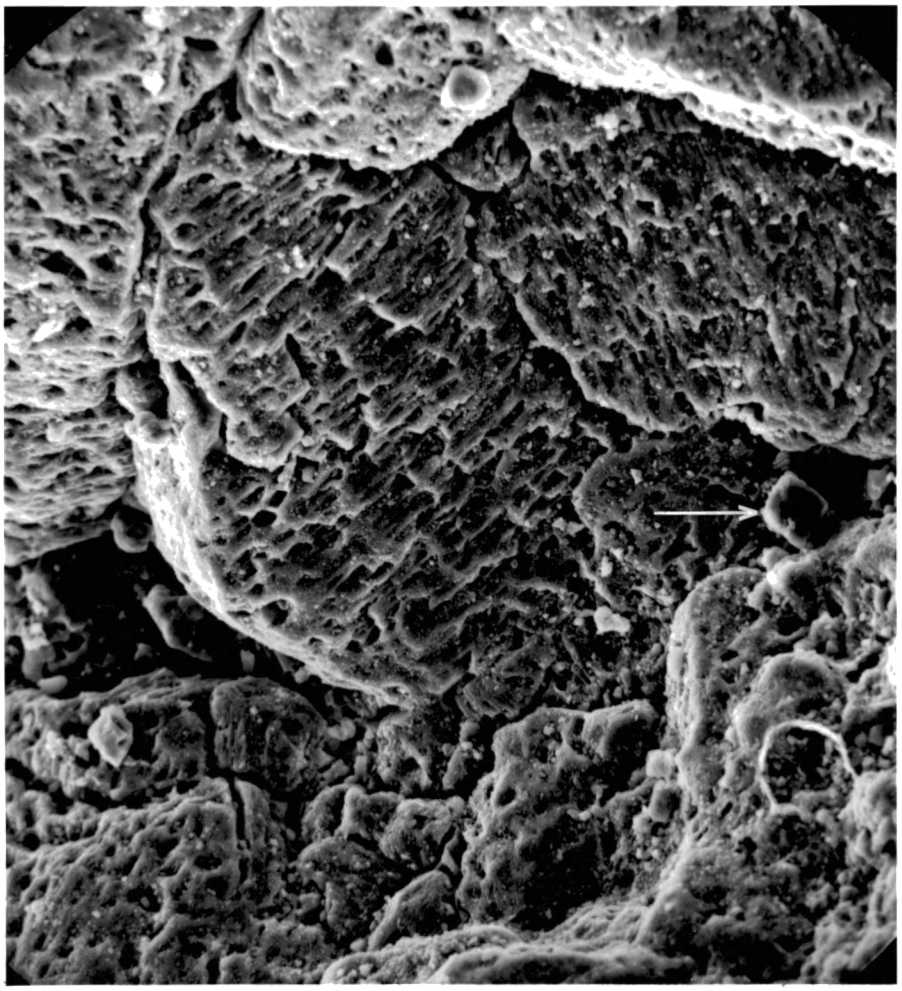

Fig. 31.-QSMFILL. Scanning electron micrograph showing an unusual secondary sparite filling. Note anhedral crystal form and the pock-marked surface texture. Rhomb-shaped crystal indicated by the arrow could be dolomite. Pock-marks could indicate some resolution, (x320).

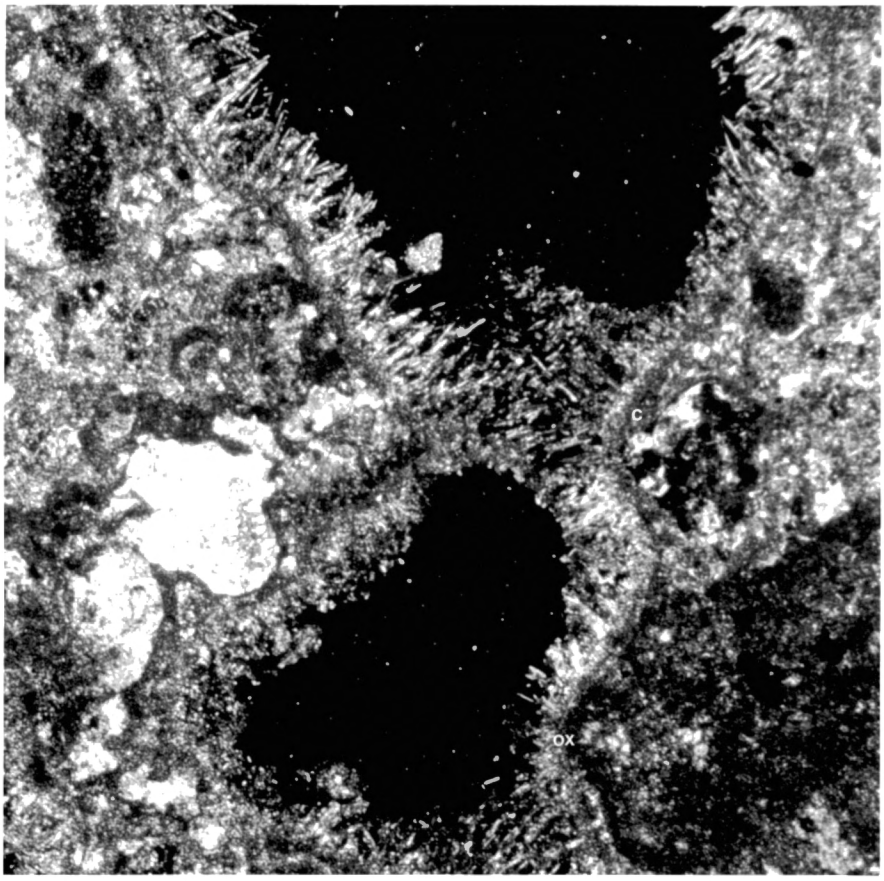

Fig. 32.-QSPI. Aragonite crystals present as pore lining. Note the distinct dark band of iron oxides (ox) and clay (c) separating the aragonite from the primary carbonate fabric. Field of view 1.66 x 2.40 mm, crossed nicols.

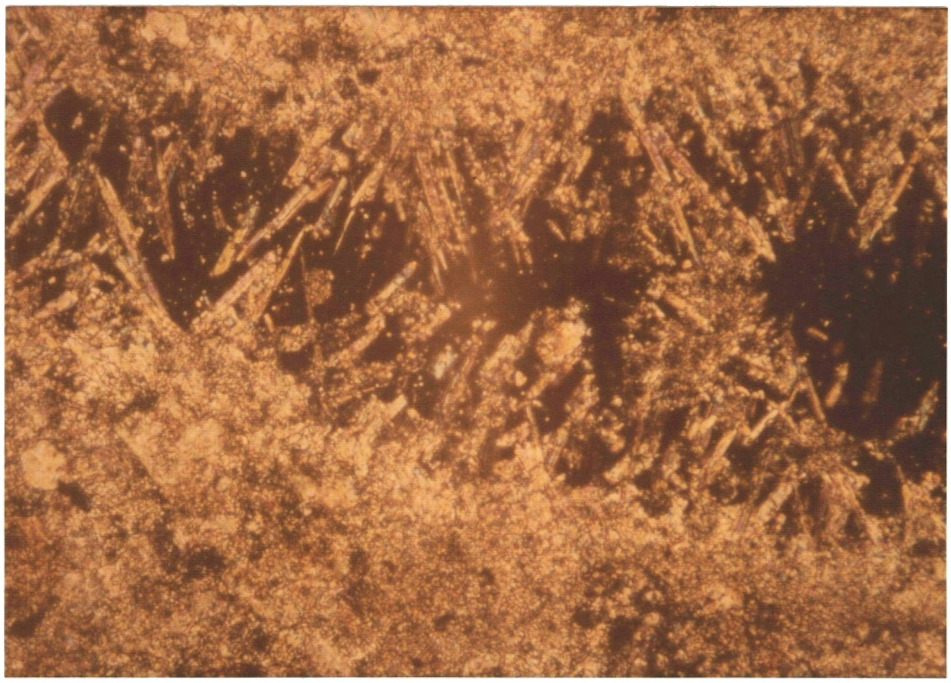

Fig. 33.-QSPI. Same as Fig. 31, but magnified to show detail. Field of view 0.45 x 0.63 mm, crossed nicols.

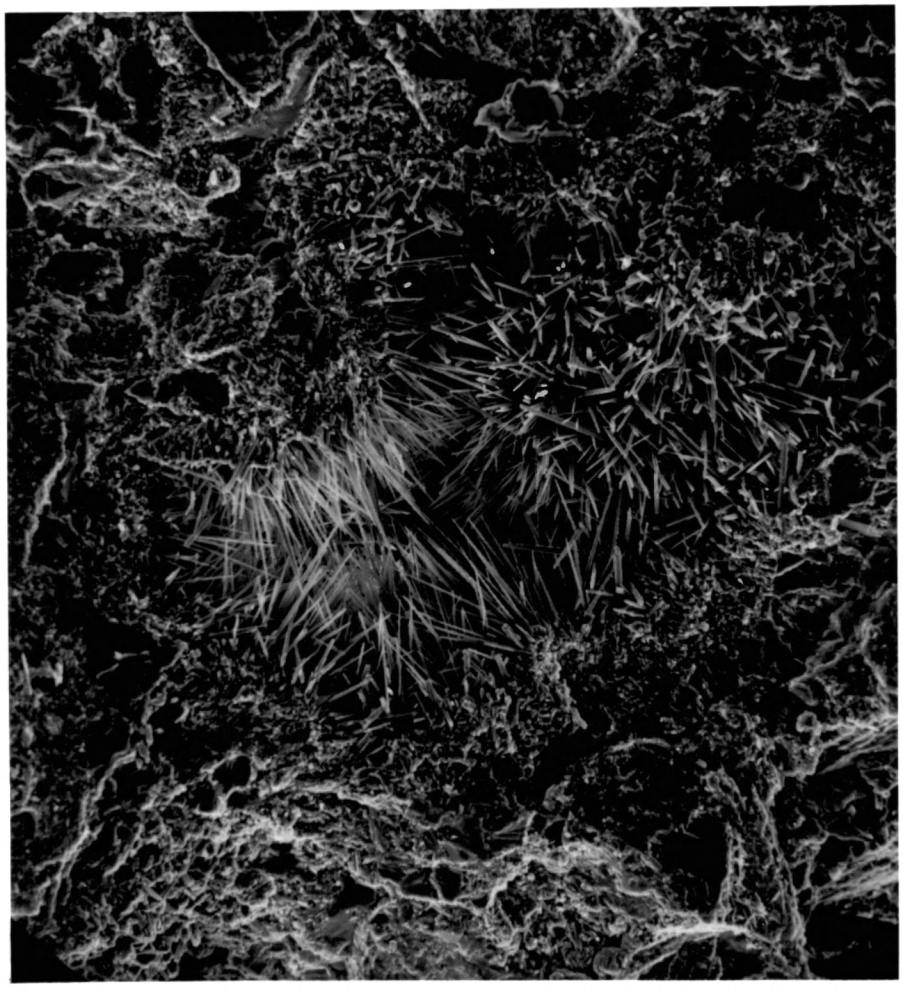

Fig. 34.-QSPI. Scanning electron micrograph of aragonite pore lining. Note anhedral character of the primary calcite fabric, (x100).

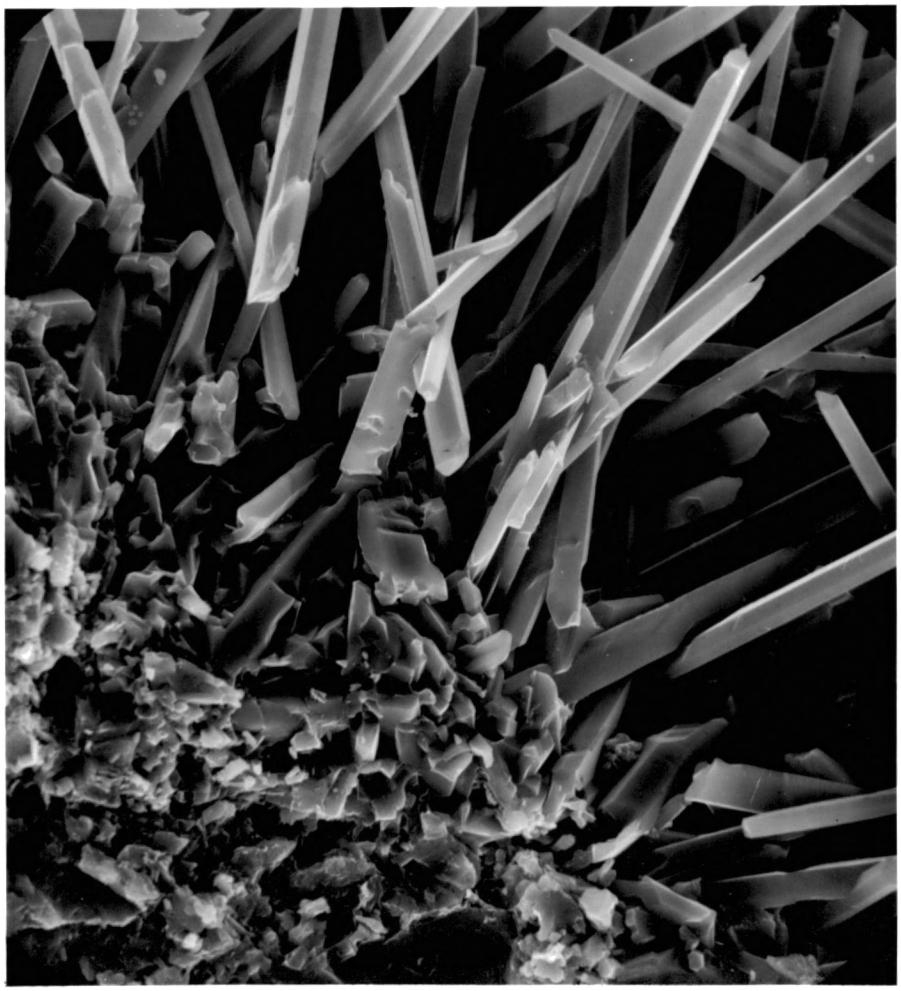

Fig. 35.-QSPI. Same as Fig. 33, but magnified to show detail of the acicular aragonite needles. Primary calcite fabric in lower left of view, (x1000).

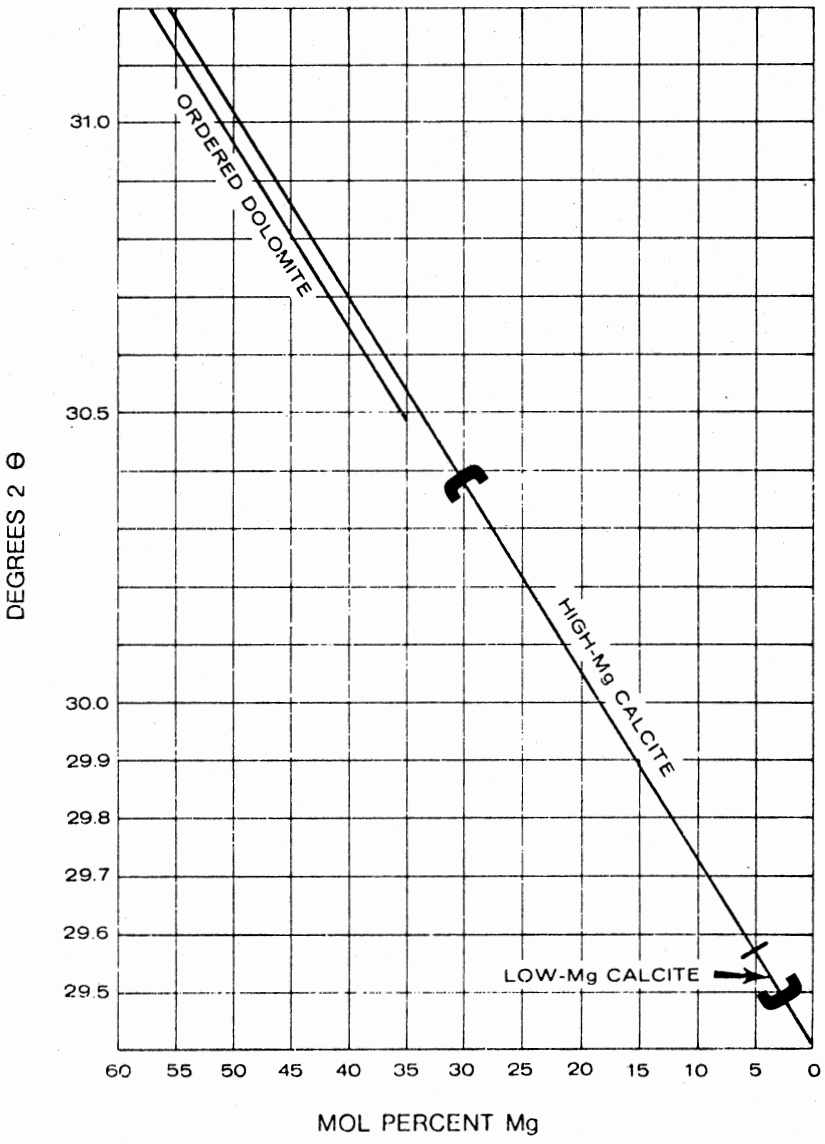

Fig. 36.-Plot of degrees 2θ versus Mol % Mg. Graph is based upon (112) reflection peak shift in carbonate rocks using X-ray diffraction. Data obtained from the present study plots along the line between the parentheses. Modified after Scholle, 1978.

The accuracy of this method is ± 0.5 Mol % Mg. In general, the results attained in this analysis were comparable with the Mg-content determined by atomic absorption spectrophotometry in all deposits except Kelly Ranch. The lack of correlation in this deposit is probably due to the influence of detrital magnesium chlorite dissolved with the carbonate.

Analysis of the insoluble residue in approximately three-quarters of the samples shows detrital quartz and feldspar (orthoclase) are usually present. Quartz invariably composes the bulk of the total residue. Hematite was found in some of the Guffy samples (material from the bottom of the spring well) and the Twin Mountains samples. None of the residues contained remaining carbonate.

Qualitative scans were made to determine the clay minerals in each of the main localities. The Kelly Ranch deposit contained the greatest amount of detrital clay, mostly iron chlorite and illite. The clay minerals at Twin Mountains consisted of kaolinite, illite, and some magnesium chlorite, with kaolinite being present in greatest abundance. Some illite was isolated in the Guffy deposit, but concentrations were nearly below instrument detection. No clay could be detected in the Soda Dam carbonate.

A few samples were X-rayed to check for possible mineralogy suggested by petrographic studies or atomic absorption analysis. Identification of aragonite was confirmed in SPI by X-ray. Two samples from Guffy were examined for strontium sulfate (celestite) and carbonate (strontianite). Neither of these minerals was found by X-ray methods, thus supporting unusual substitution of Sr^{++} for Ca^{++} in the carbonate lattice.

CHAPTER V

GEOCHEMISTRY

Introduction

Eighty-eight chemical analyses of freshwater carbonates were performed. Chemical compositions of carbonates are given in Appendix C. Correlation matrices and factor patterns for the chemical compositions of carbonates (log 10 transformed), listed separately for each main locality, are presented in Appendix D.

The geochemical data are shown in five tables, based on elemental affinities. These are:

I) Major Elements -- calcium, magnesium

II) Minor Elements (I) -- iron, manganese

III) Minor Elements (II) -- strontium, barium

IV) Alkali Elements -- sodium, potassium, lithium

V) Minor Metals -- zinc, lead, copper, chromium, nickel

These tables list the basic statistics for each of the main deposits as well as for several similar freshwater carbonate suites. In addition, the standard ratios of Mg/Ca, Sr/Ca, and Mn/Fe are listed where appropriate. Experiments have shown that these samples are drawn from log-normal distributions, but owing to custom, all statistics shown are calculated using the raw chemical data. Hence, the inordinately high values do not reflect the "true" relationships among the samples.

The terms "enrichment factor" and "maximum enrichment factor" are introduced to show a comparison between the abundance of each element in a particular deposit versus the average world-wide concentration for that element. The formulae devised for these calculations are as follows:

$$\text{Enrichment Factor} = EF_{(\text{element})} = \frac{\overline{X}_{\text{deposit}}}{\overline{X}_{\text{world}}}$$

$$\text{Maximum Enrichment Factor} = MEF_{(\text{element})} = \frac{\text{Max. Conc.}_{\text{deposit}}}{\overline{X}_{\text{world}}}$$

Further insight into the geochemistry is possible only by reducing the complex relationships among the large number of variables to simpler relationships among lesser variables. R-mode factor analysis achieves this, and since in geochemical investigations the factors produced are likely not to be independent, varimax rotation was used to produce correlating factors with the "best" interpretation of the raw data. This rotation maximizes the variance of the squared loadings on each factor separately. This tends to decrease small loadings and increase large ones. The method was employed using only the variables residue, calcium, magnesium, iron, manganese, and strontium in an effort to study the degree of bivalent cation incorporation within the carbonate lattice.

The R-mode factor analysis for the chemical data was limited to five factors for each main locality population (Appendix D). Only factors with characteristic eigenvalues >1.0 were considered significant. In all cases, these factors together accounted for at least 80% of the total variance. Individual factor loadings of 0.30 or greater

were applied toward factor identification.

Raw Chemical Data

Major Elements

Table I

The Mg/Ca- mean ratios for the four main deposits range in magnitude from 1-8. Interpreted in terms of Müller's Mg/Ca- ratio classification scheme (1969a), these deposits are categorized as follows:

Twin Mountains-- high-Mg calcite (+aragonite)

Guffy-- high-Mg calcite (+aragonite)

Kelly Ranch-- high-Mg Calcite (+aragonite)

Soda Dam-- low-Mg calcite

These relationships are generally supported by X-ray diffraction studies of the carbonate mineralogy.

The additional freshwater carbonates reflect low-Mg calcite ratios except in the case of the Corbin samples (CB). The high ratio in this deposit ($\bar{X}$=11) would classify these samples near the aragonite range, but this number is misleading, and confirmed presence of dolomite in a few specimens has lead to an inflated ratio value.

Minor Elements (I)

Table II

The individual iron and manganese values in the four main deposits are higher overall than those of the other freshwater carbonates. However, the relationship among the Mn/Fe- ratios is uniform throughout all carbonates, thus indicating a relative consistency between

TABLE I

STATISTICS FOR CALCIUM AND MAGNESIUM IN SELECTED FRESHWATER CARBONATES

(a)

Deposit		(TM) Pleistocene? Travertine Twin Mts.	(GU) Recent Travertine Guffy	(FC) Recent Travertine K. Ranch	(SD) Recent Travertine Soda Dam	(M-) Pliocene Lacustrine Verde Fm.	[1]Devonian Lacustrine	[4]Carbonate World-Average
N		26	12	8	6	4	7	
Calcium, Ca	$\bar{X}$	317200	303900	285100	327500	314800	-	302300
	S_x	55540	84929	41212	12406	17651	-	
	EF	1.04	1.00	0.94	1.08	1.04	-	
Magnesium, Mg	$\bar{X}$	6326	8602	8997	2593	3218	-	47000
	S_x	4081	4685	5916	1197	1141	-	
	EF	0.14	0.18	0.19	0.06	0.07	-	
	MEF	0.49	0.40	0.39	0.09	0.10	-	
Mg/Ca-ratio	$\bar{X}$	3	8	5	1	1.70	-	
	R	1-11	2-49	2-12	0.7-2	1-2	-	

TABLE I (Continued)

(b)

Deposit		[2]Recent Lacustrine	[3]Pleistocene? Travertine T. Falls	[3]Recent Travertine T. Falls	[3]Recent Travertine Malham	(CB) Permian Paleosoil Corbin	(K-) Devonian Paleosoil Cornstones	[4]Carbonate World-Average
N		11	24	11	14	10	13	
Calcium, Ca	$\bar{X}$	-	303900	312400	268000	314800	293400	302300
	S_x	-	31806	27296	11287	91907	38869	
	EF	-	1.00	1.03	0.87	1.04	0.97	
	MEF	-	1.18	1.16	0.95	1.54	1.32	
Magnesium, Mg	$\bar{X}$	-	1519	1089	118	12743	2771	47000
	S_x	-	575	466	29	23249	2646	
	EF	-	0.03	0.02	0.003	0.27	0.06	
	MEF	-	0.07	0.03	0.003	1.64	0.22	
Mg/Ca-ratio	$\bar{X}$	-	0.81	0.56	0.07	11	1	
	R	-	0.35-1.47	0.19-0.83	0.03-0.09	0.89-80	0.73-5.24	

Values expressed as concentrations (ppm) in HCl soluble fraction
* = whole rock concentrations; acetic acid dissolution
( ) = number of samples analyzed, if different from N
EF = enrichment factor MEF = maximum enrichment factor
R = range nd = not detectable
$\bar{X}$ = mean S_x = standard deviation

[1]Donovan (unpub. data)
[2]Deurer et al. (1978)
[3]Armstrong (unpub. data)
[4]Rosler and Lange (1972)

TABLE II

STATISTICS FOR IRON AND MANGANESE IN
SELECTED FRESHWATER CARBONATES

(a)

Deposit		(TM) Pleistocene? Travertine Twin Mts.	(TU) Recent Travertine Guffy	(FC) Recent Travertine K. Ranch	(SD) Recent Travertine Soda Dam	(M-) Pliocene Lacustrine Verde Fm.	[1]Devonian Lacustrine	[4]Carbonate World Average
N		26	12	8	6	4	7	
Iron, Fe	$\bar{X}$	1714	23696	14606	540	1063	-	3800
	S_x	1257	38262	17528	169	506	-	
	EF	0.45	6.24	3.84	0.14	0.28	-	
	MEF	1.77	27.63	13.83	0.20	0.46	-	
Manganese, Mn	$\bar{X}$	251	430	1332	1074	273	-	1100
	S_x	337	312	2039	622	456	-	
	EF	0.23	0.39	1.21	0.98	0.29	-	
	MEF	1.01	1.17	5.58	1.52	0.87	-	
Mn/Fe-ratio	$\bar{X}$	15	12	33	195	27	-	
	R	2-83	0.18-70	2-219	4-355	4-94	-	

TABLE II (Continued)

(b)

Deposit		[2]Recent Lacustrine	[3]Pleistocene? Travertine T. Falls	[3]Recent Travertine T. Falls	[3]Recent Travertine Malham	(CB) Permian Paleosoil Corbin	(K-) Devonian Paleosoil Cornstones	[4]Carbonate World-Average
N		11	24	11	14	10	13	
Iron, Fe	$\bar{X}$	1470	807	686	308	1248	1479	3800
	S_x	999	838	887	132	1066	997	
	EF	0.39	0.21	0.18	0.08	0.33	0.39	
	MEF	0.74	0.73	0.87	0.13	0.95	0.97	
Manganese, Mn	$\bar{X}$	228	147	130	36	515	1583	1100
	S_x	151	121	53	18	351	640	
	EF	0.21	0.13	0.12	0.03	0.49	1.44	
	MEF	0.44	0.37	0.21	0.05	1.06	2.25	
Mn/Fe-ratio	$\bar{X}$	16	25	33	13	56	123	
	R	0-244	7-65	3-59	1-22	16-118	20-283	

Values expressed as concentrations (ppm) in HCl soluble fraction
* = whole rock concentrations; acetic acid dissolution
( ) = number of samples analyzed, if different from N
EF = enrichment factor MEF = maximum enrichment factor
R = range nd = not detectable
$\bar{X}$ = mean S_x = standard deviation

[1]Donovan (unpub. data)
[2]Deurer et al. (1978)
[3]Armstrong (unpub. data)
[4]Rosler and Lange (1972)

these elements irresponsive to selective enrichment for a particular deposit.

In comparison to Müller's study (1971), good agreement is found among Mn/Fe- ratios of these specimens and the rocks in the present investigation.

Minor Elements (II)

Table III

In all deposits, the Sr/Ca- mean ratios determined correspond closely with previous investigations on similar freshwater rock-types (Müller, 1969a; Irion and Müller, 1968b). Only the Guffy deposit is atypically high in magnitude, but this value may reflect strontium contributions from a sulfate phase (celestite).

Barium is greatly enriched in all deposits. This could indicate sulfate contributions (barite) and/or constituents adsorbed in clay.

Alkali Elements

Table IV

The alkalis are present in generally below average concentrations in comparison to the world average for carbonates. Only sodium shows a consistent enrichment in some deposits, possibly owing to sulfate (thenardite) and/or chloride (halite) contributions.

Minor Metals

Table V

Overall, the minor metals are enriched in all cases excluding chromium, nickel, and at some localities, zinc. There are some

TABLE III

STATISTICS FOR STRONTIUM AND BARIUM IN SELECTED FRESHWATER CARBONATES

(a)

Deposit		(TM) Pleistocene? Travertine Twin Mts.	(GU) Recent Travertine Guffy	(FC) Recent Travertine K. Ranch	(SD) Recent Travertine Soda Dam	(M-) Pliocene Lacustrine Verde Fm.	[1]Devonian Lacustrine	[4]Carbonate World-Average
N		26	12	8	6	4	7	
Strontium, Sr	$\bar{X}$	190	4862	569	296	242	2060	610
	S_x	109	1913	396	221	81	1456	
	EF	0.31	7.97	0.93	0.49	0.40	3.38	
	MEF	0.98	14.09	1.93	1.19	0.52	8.10	
Barium, Ba	$\bar{X}$	154	185	363	374	426	-	10
	S_x	100	190	262	274	202	-	
	EF	15.40	18.50	36.30	37.40	42.60	-	
	MEF	43.50	76.40	87.00	78.10	62.50	-	
Sr/Ca-ratio	$\bar{X}$	0.27	9	1	0.41	0.35	-	
	R	0.16-0.75	2-28	0.34-2	0.15-1	0.19-0.42	-	

TABLE III (Continued)

(b)

Deposit		[2]Recent Lacustrine	[3]Pleistocene? Travertine T. Falls	[3]Recent Travertine T. Falls	[3]Recent Travertine Malham	(CB) Permian Paleosoil Corbin	(K-) Devonian Paleosoil Cornstones	[4]Carbonate World-Average
N		11	24	11	14	10	13	
Strontium, Sr	$\bar{X}$	-	267	320	49	450	241	610
	S_x	-	87	48	11	563	62	
	EF	-	0.44	0.52	0.08	0.74	0.40	
	MEF	-	0.77	0.63	0.13	2.84	0.52	
Barium, Ba	$\bar{X}$	-	167(11)	148(8)	80(7)	352	74	10
	S_x	-	73	33	49	272	88	
	EF	-	16.70	14.80	8.00	35.20	7.40	
	MEF	-	35.60	20.60	15.20	74.10	24.40	
Sr/Ca-ratio	$\bar{X}$	-	0.40	0.47	0.08	0.93	0.33	
	R	-	0.25-0.67	0.36-0.56	0.04-0.12	0.12-5	0.25-0.52	

Values expressed as concentrations (ppm) in HCl soluble fraction
* = whole rock concentrations; acetic acid dissolution
( ) = number of samples analyzed, if different from N
EF = enrichment factor MEF = maximum enrichment factor
R = range nd = not detectable
$\bar{X}$ = mean S_x = standard deviation

[1]Donovan (unpub. data)
[2]Deurer et al. (1978)
[3]Armstrong (unpub. data)
[4]Rosler and Lange (1972)

TABLE IV

STATISTICS FOR SODIUM, POTASSIUM, AND LITHIUM IN SELECTED FRESHWATER CARBONATES

(a)

Deposit		(TM) Pleistocene? Travertine Twin Mts.	(GU) Recent Travertine Guffy	(FC) Recent Travertine K. Ranch	(SD) Recent Travertine Soda Dam	(M-) Pliocene Lacustrine Verde Fm.	[1]Devonian Lacustrine	[4]Carbonate World-Average
N		26	12	8	6	4	7	
Sodium, Na	$\bar{X}$	327	1694	747	478	611	-	400
	S_x	126	674	261	167	78	-	
	EF	0.81	4.24	1.87	1.20	1.53	-	
	MEF	1.39	8.81	2.69	1.69	1.81	-	
Potassium, K	$\bar{X}$	191	884	946	118	212	-	2700
	S_x	123	1351	881	96	86	-	
	EF	0.07	0.33	0.35	0.04	0.08	-	
	MEF	0.16	1.83	0.95	0.96	0.11	-	
Lithium, Li	$\bar{X}$	3	19	6	12	12	nd	5-20
	S_x	3	10	5	5	0.96	-	
	EF	0.15-0.60	0.95-3.80	0.30-1.20	0.60-2.40	0.60-2.40	-	
	MEF	0.90-3.60	2.15-8.60	0.65-2.60	0.95-3.80	0.65-2.60	-	

TABLE IV (Continued)

(b)

Deposit		[2]Recent Lacustrine	[3]Pleistocene? Travertine T. Falls	[3]Recent Travertine T. Falls	[3]Recent Travertine Malham	(CB) Permian Paleosoil Corbin	(K-) Devonian Paleosoil Cornstones	[4]Carbonate World-Average
N		11	24	11	14	10	13	
Sodium, Na	$\bar{X}$	-	151	102	14	1498	416	400
	S_x	-	186	93	51	969	266	
	EF	-	0.38	0.26	0.035	3.75	0.033	
	MEF	-	0.22	0.08	0.06	7.20	2.68	
Potassium, K	$\bar{X}$	-	170	64	5	383	385	2700
	S_x	-	243	36	12	242	262	
	EF	-	0.06	0.02	0.002	0.14	0.14	
	MEF	-	0.40	0.05	0.02	0.28	0.42	
Lithium, Li	$\bar{X}$	-	1 (13)	1 (8)	nd (8)	4	2	5-20
	S_x	-	1	1	-	3	0.66	
	EF	-	0.05-0.20	0.05-0.20	-	0.20-0.80	0.10-0.40	
	MEF	-	0.10-0.40	0.50-2.00	-	0.50-5.00	0.15-0.60	

Values expressed as concentrations (ppm) in HCl soluble fraction
* = whole rock concentrations; acetic acid dissolution
( ) = number of samples analyzed, if different from N
EF = enrichment factor MEF = maximum enrichment factor
R = range nd = not detectable
$\bar{X}$ = mean S_x = standard deviation

[1]Donovan (unpub. data)
[2]Deurer et al. (1978)
[3]Armstrong (unpub. data)
[4]Rosler and Lange (1972)

TABLE V

STATISTICS FOR ZINC, LEAD, COPPER, CHROMIUM, AND NICKEL
IN SELECTED FRESHWATER CARBONATES

(a)

Deposit		(TM) Pleistocene? Travertine Twin Mts.	(GU) Recent Travertine Guffy	(FC) Recent Travertine K. Ranch	(SD) Recent Travertine Soda Dam	(M-) Pliocene Lacustrine Verde Fm.	[1]Devonian Lacustrine	[4]Carbonate World-Average
N		26	12	8	6	4	7	
Zinc, Zn	$\bar{X}$	113	48	72	27	38	11	20
	S_x	36	42	103	42	33	6	
	EF	5.65	2.40	3.60	1.35	1.90	0.55	
	MEF	9.35	8.30	16.15	5.55	4.35	1.10	
Lead, Pb	$\bar{X}$	35	48	45	39	38	12	9-27
	S_x	7	27	11	6	9	5	
	EF	1.30-5.00	1.78-5.33	1.67-5.00	1.44-4.33	1.41-4.22	0.44-1.33	
	MEF	1.74-5.22	4.63-13.89	2.22-6.67	1.70-5.11	1.89-5.67	0.71-2.11	
Copper, Cu	$\bar{X}$	40	26	40	27	26	72	4
	S_x	19	13	14	15	0	145	
	EF	10.00	6.50	10.00	6.75	6.50	18.00	
	MEF	24.00	15.75	16.50	12.75	6.50	100.00	

TABLE V (Continued)

(a) (Continued)

Deposit		(TM) Pleistocene? Travertine Twin Mts.	(GU) Recent Travertine Guffy	(FC) Recent Travertine K. Ranch	(SD) Recent Travertine Soda Dam	(M-) Pliocene Lacustrine Verde Fm.	[1]Devonian Lacustrine	[4]Carbonate World-Average
N		26	12	8	6	4	7	
Chromium, Cr	$\bar{X}$	59	8	8	6	5	nd	11
	S_x	76	8	4	0.83	0	-	
	EF	5.36	0.73	0.73	0.55	0.45	-	
	MEF	23.00	2.82	1.18	0.64	0.45	-	
Nickel, Ni	$\bar{X}$	31	13	19	21	24	nd	20
	S_x	30	13	12	20	6	-	
	EF	1.55	0.65	0.95	1.05	1.20	-	
	MEF	4.95	2.10	1.90	2.65	1.55	-	

TABLE V (Continued)

(b)

Deposit		[2]Recent Lacustrine	[3]Pleistocene? Travertine T. Falls	[3]Recent Travertine T. Falls	[3]Recent Travertine Malham	(CB) Permian Paleosoil Corbin	(K-) Devonian Paleosoil Cornstones	[4]Carbonate World-Average
N		11	24	11	14	10	13	
Zinc, Zn	$\bar{X}$	28	7	11	175	17	10	20
	S_x	29	2	10	72	11	3	
	EF	1.40	0.35	0.55	8.75	0.85	0.50	
	MEF	5.40	0.65	2.15	13.65	2.25	0.85	
Lead, Pb	$\bar{X}$	-	41(16)	43(8)	44(7)	44	47	9-27
	S_x	-	6	6	3	11	7	
	EF	-	1.52-4.56	1.60-4.78	1.63-4.89	1.63-4.89	1.74-5.22	
	MEF	-	2.07-6.22	2.07-6.22	1.85-5.56	2.33-7.00	2.07-6.22	
Copper, Cu	$\bar{X}$	5	6(12)	6(5)	5(5)	59	19	4
	S_x	5	2	2	0	84	4	
	EF	1.25	1.50	1.50	1.25	14.75	4.75	
	MEF	3.75	2.75	2.50	1.25	69.50	6.50	

TABLE V (Continued)

(b) (Continued)

Deposit		[2]Recent Lacustrine	[3]Pleistocene? Travertine T. Falls	[3]Recent Travertine T. Falls	[3]Recent Travertine Malham	(CB) Permian Paleosoil Corbin	(K-) Devonian Paleosoil Cornstones	[4]Carbonate World-Average
N		11	24	11	14	10	13	
Chromium, Cr	$\bar{X}$	0.22	5(11)	5(8)	5(5)	7	5	11
	S_x	0.60	0	2	0	3	3	
	EF	0.02	0.45	0.45	0.45	0.64	0.45	
	MEF	0.18	0.45	0.91	0.45	1.09	0.73	
Nickel, Ni	$\bar{X}$	-	-	-	-	13	6	20
	S_x	-	-	-	-	8	6	
	EF	-	-	-	-	0.65	0.30	
	MEF	-	-	-	-	1.50	0.90	

Values expressed as concentrations (ppm) in HCl soluble fraction
* = whole rock concentrations; acetic acid dissolution
( ) = number of samples analyzed, if different from N
EF = enrichment factor MEF = maximum enrichment factor
R = range nd = not detectable
$\bar{X}$ = mean S_x = standard deviation

[1]Donovan (unpub. data)
[2]Deurer et al. (1978)
[3]Armstrong (unpub. data)
[4]Rosler and Lange (1972)

exceptions (particularly with regard to Twin Mountains), but generally the metals are abundant constituents probably related to detrital contamination.

Mathematical Model

The Hypothesis of Lognormality and Testing Methods

The populations being considered here may be approximated by some kind of frequency distribution. The assumption is stated at this point that the underlying distribution of the hypothetical populations, elemental compositions of all hydrothermal "freshwater" carbonates, if randomly sampled with large samples (N >50), could be shown to be approximated by one of the continuous theoretical distributions. For purposes of testing the assumption just stated, the hypothesis is advanced that the distribution of the hypothetical populations could be approximated by the lognormal distribution. This assumption is based upon the premise that, in most cases, geological phenomena are approximated most effectively by the lognormal distribution (Griffiths, 1967).

Undeniably, the sample sizes under study are small bases for generalizations about populations; but in this instance they are the total populations available for study. There are several methods for testing of hypotheses asserting normality of a population (i.e., mean and variance of the sample, histogram construction, Chi-square goodness-of-fit test, skewness and kurtosis, to name a few). For purposes of this study, the Kolmogorov-Smirnov test for goodness-of-fit

was utilized because it can be applied to populations consisting of exceptionally small sample sizes. If the Kolmogorov-Smirnov D_{max} values exceed the critical values at a level of probability set by the investigator, the null hypothesis is rejected, and an alternate hypothesis is adopted for testing (Miller and Kahn, 1962). The alternate hypothesis may assume a) that the underlying distribution is not approximated by the lognormal distribution with the given parameters, b) that the underlying distribution might be approximated by some other distribution if the variates were transformed differently, or c) that the sampling method did not yield a truly random sample. Testing proceeds in this fashion until the results indicate acceptable consistency between the distribution suggested by the sample and some theoretical distribution.

Tests for Lognormality of the Populations

The null hypothesis is:

H_o: The elements under inspection are random samples from a lognormally distributed population.

Alternate hypotheses are:

H_1: The elements under inspection are random samples from a non-lognormally distributed population.

H_2: The elements under inspection are non-random samples from a lognormally distributed population.

H_3: The elements under inspection are non-random samples from a non-lognormally distributed population.

If any of the computed values of D_{max} of the Kolmogorov-Smirnov test are larger than their corresponding tabled critical values, the appropriate null hypothesis is rejected. If the null hypothesis is rejected, one of the alternate hypotheses is assumed to be true, but

distinction among the separate alternate hypotheses is unwarranted.

The conclusions follow from the statistics in Table VI that on the basis of assumptions used in this testing (i.e., that in this case, the Kolmogorov-Smirnov test is sufficient to isolate biased samples), no reason exists to reject the null hypothesis ($\alpha = 0.05$); elemental compositions of all hydrothermal "freshwater" carbonates, are presumed to be approximated by lognormal distributions of which the sample means ($\bar{X}$) and standard deviations (S_x) are estimates of the populations' true means (μ) and standard deviations (σ_x).

Factor Analysis

In the following analysis, the role of Ca is interpreted entirely in terms of the calcium-carbonate mineralogy. Although the $CO_3^{=}$ anion was not analyzed for, petrographic and X-ray diffraction studies failed to isolate any other mineral that might contribute significant Ca to the chemical system. Discussion is keyed to Appendix D.

Twin Mountains

Factor 1. The very high positive loading on Fe and the moderate positive loading on Mn reflect contributions in the form of oxides of these elements, thus this factor should be designated "the oxide contamination factor." The stratigraphic positioning of this deposit above the "red-bed" Fountain Formation supports this identification based upon the red coloration of many of the travertine samples. Although one might suspect a significant positive loading on the residue variate in this situation, lack of this agreement is easily

TABLE VI

SUMMARY STATISTICS, TEST FOR LOGNORMALITY OF ELEMENTAL COMPOSITIONS*

	Residue	Ca	Mg	Fe	Mn	Sr
Twin Mts.						
N=26						
$\bar{X}$	-1.36	5.49	3.75	3.14	2.09	2.27
S_x	0.62	0.09	0.21	0.31	0.62	0.21
K-S D_{max}, calc.	.13401	.20535	.10506	.15266	.09178	.13497
K-S D_{max}, crit.**	.25907	.25907	.25907	.25907	.25907	.25907
Guffy						
N=12						
$\bar{X}$	-1.37	5.45	3.88	3.84	2.55	3.65
S_x	0.67	0.24	0.24	0.74	0.28	0.21
K-S D_{max}, calc.	.13283	.33869	.24254	.17122	.11623	.14910
K-S D_{max}, crit.	.37543	.37543	.37543	.37543	.37543	.37543
Kelly Ranch						
N=8						
$\bar{X}$	-0.76	5.45	3.85	3.89	2.81	2.66
S_x	0.66	0.06	0.33	0.56	0.51	0.30
K-S D_{max}, calc.	.20274	.12075	.19944	.12184	.32204	.22166
K-S D_{max}, crit.	.45427	.45427	.45427	.45427	.45427	.45427
Soda Dam						
N=6						
$\bar{X}$	-1.71	5.51	3.38	2.71	2.74	2.39
S_x	0.51	0.02	0.20	0.15	0.86	0.28
K-S D_{max}, calc.	.12986	.15494	.22524	.12418	.28924	.27505
K-S D_{max}, crit.	.51926	.51926	.51926	.51926	.51926	.51926

*Level of significance, 0.05. Variables measured in $\log_{10}$ of parts per million.

**K-S D_{max} critical values taken from Miller and Kahn, 1962.

explained by partial dissolution of the oxide constituents during the HCl digestion process.

Factor 2. With the very high positive loading on Ca and high positive loading on Sr, this factor justifies the name "carbonate factor." Fig. 37 shows the excellent correlation between this factor and the Ca variate. This agreement between Ca and Sr suggests a relatively high degree of Sr^{++} incorporation into the calcium carbonate lattice. This indication has not been supported by X-ray identification of $SrCO_3$ (strontianite) as such, but the confirmed presence of aragonite in some samples (e.g. SPI), with its known affinity for Sr^{++} incorporation into its structure (Lippmann, 1973), suggests that aragonite may be present in greater abundance in this deposit than as indicated by the present study. Strength of this factor probably represents periods of minimal erosion with little detrital contamination.

Factor 3. This factor may be identified as the "clay contamination factor" based upon the single very high loading on Mg. The presence of magnesium chlorite has been established by X-ray diffraction, and dissolution of chlorite clay by HCl is probable, based on known solubility relationships.

Guffy

Factor 1. Factor 1 is slightly bipolar with very high positive loadings on residue and Fe and an associated low positive loading on Mn opposed to low negatively loaded Ca. This obviously reflects the antipathetic relationship between detrital sediments on the one hand and the calcium carbonate on the other. A plot of Factor 1 versus

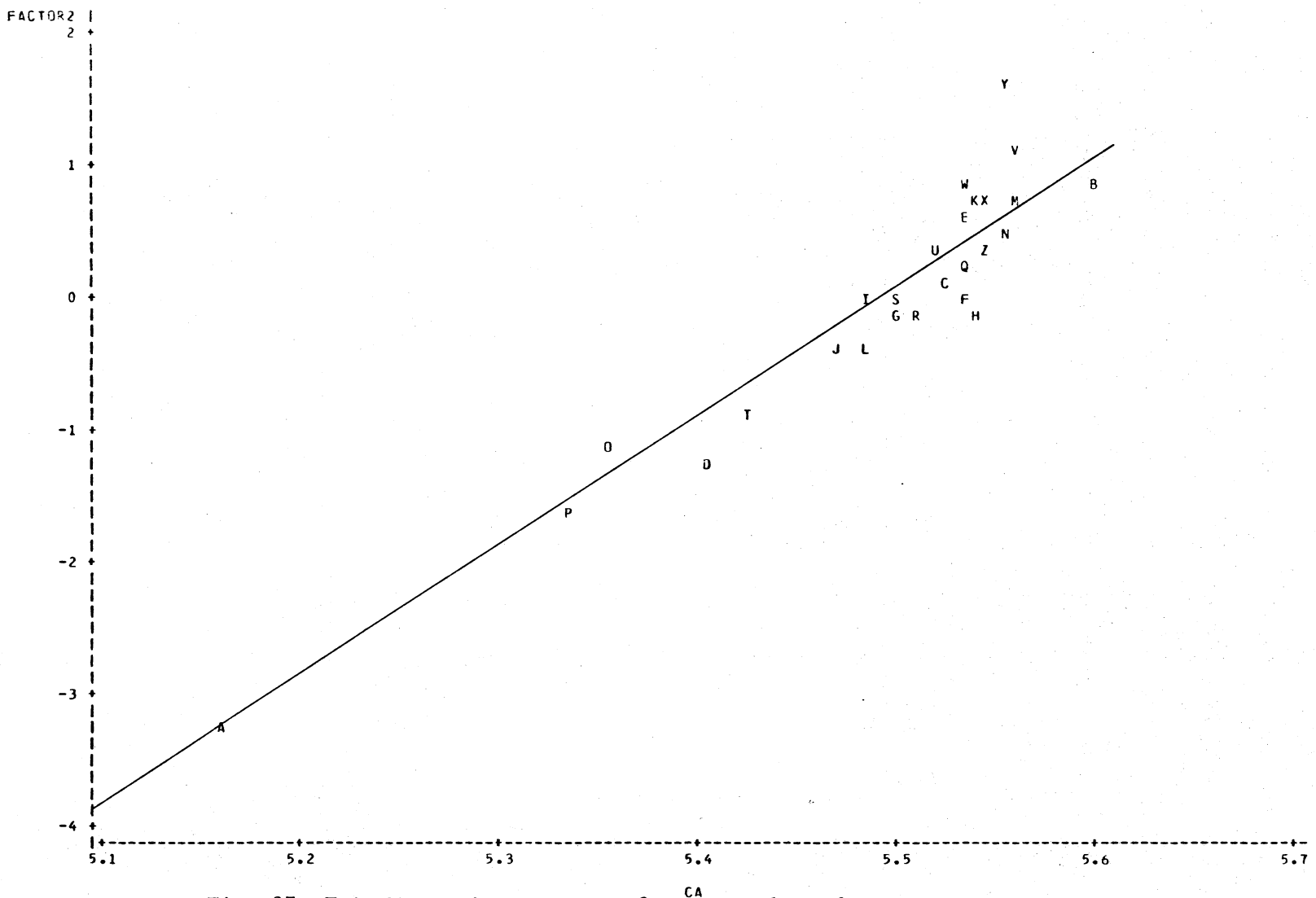

Fig. 37.-Twin Mountains. Factor 2 scores plotted against Ca variate. Symbol is individual sample identification.

residue (Fig. 38) shows a reasonably strong correlation, thus the designation of "sediment contamination factor" is proposed.

This deposit is located adjacent to a Tertiary volcanic complex (i.e., the Guffy Caldera). Hence enrichment of Fe and Mn in the detrital sediments is to be expected.

Factor 2. Very high positive loadings on Mg and Sr coupled with low negatively loaded Fe suggests that this factor may be named "the sulfate factor." The minerals celestite ($SrSO_4$) and epsomite ($MgSO_4 \cdot 7H_2O$) may be found associated with "cave-type" deposits. Although these minerals were not detected by X-ray diffraction, and the $SO_4^{=}$ anion was not analyzed for, the Guffy spring is a plausible site for sulfate precipitation. Factor 2 might be influenced by paleoclimatic conditions of increased aridity.

Kelly Ranch

Factor 1. Factor 1 is truly bipolar with a very high negative loading on calcium versus very high positive loadings on residue and Fe. This antipathetic relationship reflects the contribution of significant amounts of iron chlorite from the Cretaceous shale bedrock. X-ray diffraction has identified iron chlorite to be present in relatively high quantities, and petrographic examination supports the incorporation of clay detritus within the calcite fabric. Factor 1 has isolated the detrital phase--precipitated phase relationship, so the name "clay contamination factor" is proposed.

Factor 2. Identification of Factor 2 is puzzling upon initial investigation. Very high negative loadings on Mg and Sr with associated low negatively loaded residue dominate the factor. Two possible

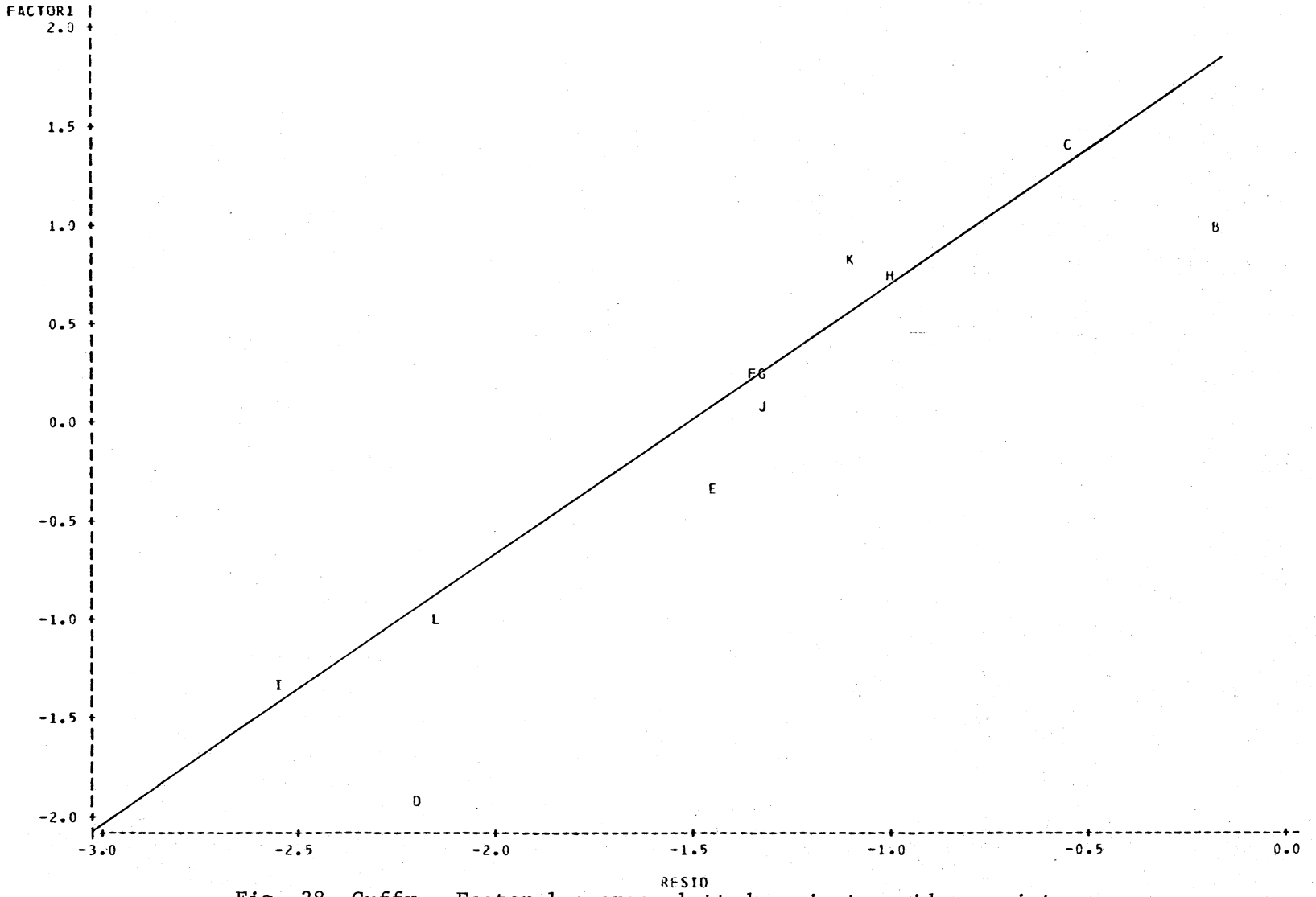

Fig. 38.-Guffy. Factor 1 scores plotted against residue variate. Symbol is individual sample identification.

interpretations of these relationships are presented. Foremost, the likelihood of sulfate minerals of these elements is considered. Clearly, such an interpretation is more easily understood if based upon the oxidizing conditions under which the rocks were formed. Periods of maximal aridity and minimal erosion might play an important role. Secondly, Mg and Sr contributed as interlamellar cations in detrital clay is possible. Although this interpretation lacks evidence, the correlation of the residue variate coupled with the confirmed presence of illite within the calcite fabric affords some creditability to this hypothesis of clay contamination.

Due to the dual interpretation of this factor, no formal name will be applied.

Soda Dam

Factor 1. An obvious bimodal distribution is displayed, based upon a very high negatively loaded residue versus a very high positively loaded Ca and associated low loaded Fe. This factor clearly illustrates the antipathetic relationship between the precipitated calcium carbonate and the contribution of detrital constituents. In addition, the weak correlation between Ca and Fe suggests some degree of Fe incorporation into the calcite lattice. Factor 1 is thus designated "the carbonate factor" based on these relationships. Fig. 39 plots Factor 1 versus calcium. Correlation is good; the line drawn is believed to represent the most realistic regression.

Factor 2. Very high positive loadings on Fe and Mn suggest an "oxide contamination factor" is present. Lack of significant loading on residue in this factor may be interpreted similarly to the "oxide

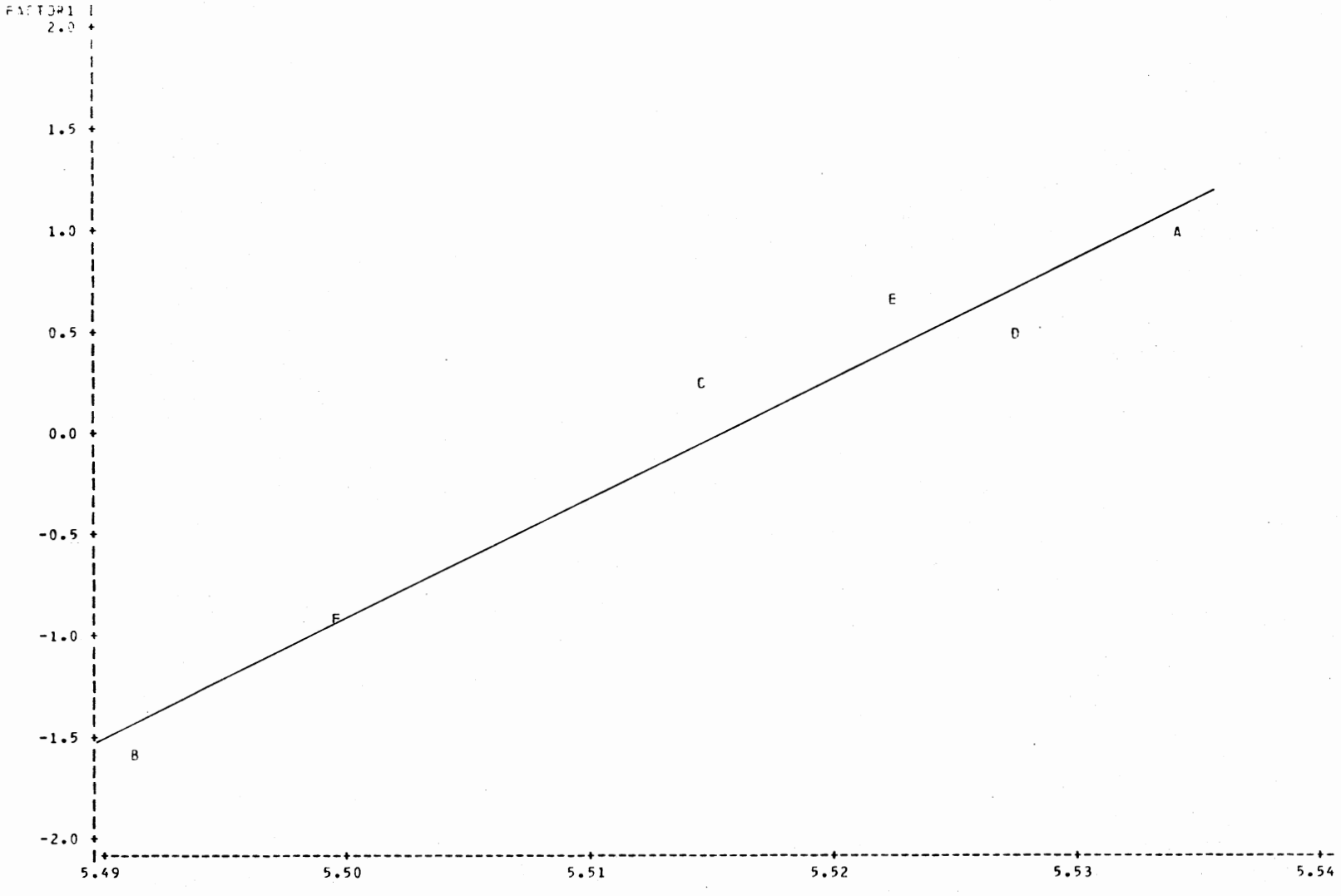

Fig. 39.-Soda Dam. Factor 1 scores plotted against Ca variate. Symbol is individual sample identification.

factor" at Twin Mountains (Factor 1, p. 72).

Factor 3. Factor 3 is assigned the name "volcanic enrichment factor." This deposit is situated along a ring fault associated with the Valles Caldera. The volcanics in this area are enriched in Mg and depleted in Mn (Trainer, 1974). The very high positive loading on Mg as opposed to the low negative loading on Mn clearly reflects the composition of the volcanics. Whether contributions are the result of bedrock erosion or contemporaneous enrichment during carbonate precipitation is indeterminable from this study.

CHAPTER VI

SUMMARY

The following principal conclusions may be drawn from this study:

1) The Twin Mountains, Guffy, Kelly Ranch, and Soda Dam localities are examples of hydrothermal "freshwater" carbonate deposits.
2) Local topography, seasonal climatic change, and flow rate all contribute to the character of the spring deposit formed.
3) Ellipsoidal buildups with high depositional dips, travertine terraces, and terracettes are characteristic features of some hydrothermal "freshwater" carbonates.
4) The dominant carbonate fabric is a mozaic of anhedral equigranular micrite and microsparite that forms an irregular spongy texture.
5) Primary carbonate mineralogy ranges from low-Mg calcite to high-Mg calcite (+aragonite).
6) Incorporation of bivalent cations, particularly Sr^{++}, into the calcium carbonate lattice is a common feature.
7) The frequency distribution of the freshwater carbonate populations in this study are suitably approximated by the lognormal distribution.
8) R-mode factor analysis reasonably defines the important interrelationships of elements and allows further insight into the

geochemistry of the carbonates.

9) Application of chemical equilibria relationships is difficult owing to the incorporation of detrital materials during carbonate precipitation.

10) In general, carbonate chemistry is influenced by and reflects the composition of the bedrock.

11) Further research should consider alternative methods for digestion of rock, so as to minimize contamination.

BIBLIOGRAPHY

Alderman, A. R., and C. C. Von der Borch, 1960, Occurrence of hydrothermal magnesite in sediments in South Australia: Nature, v. 188, p. 931.

_____, 1963, A dolomite reaction series: Nature, v. 198, p. 465-466.

Angino, E. E., and G. K. Billings, 1972, Atomic absorption spectrometry in geology: New York, Elsevier, 191 p.

Armstrong, J. R., 1978, Geochemical and petrologic characteristics of selected freshwater limestones: Unpub. M. S. thesis, Oklahoma State Univ.

Bathurst, R. G. C., 1968, Precipitation of oöids and other aragonite fabrics in warm seas, in Müller, G., and G. M. Friedman (eds.), Recent developments in carbonate sedimentology in Central Europe: New York, Springer-Verlag, p. 1-10.

_____, 1975, Carbonate sediments and their diagenesis, Developments in sedimentology, v. 12: New York, Elsevier, 658 p.

Baltres, A., 1975, Lithification of some modern carbonate sediments in a hypersaline lake adjacent to the Black Sea: Sediment. Geol., v. 13, p. 291-302.

Bausch, W. M., 1965, Strontiumgehalte in süddeutschen Malmkalken: Geol. Rundschau, v. 55, p. 86-96.

_____, 1968a, Clay content and calcite crystal size in limestones: Sedimentology, v. 10, p. 71-75.

_____, 1968b, Outlines of distribution of strontium in marine limestones, in Müller, G., and G. M. Friedman (eds.), Recent developments in carbonate sedimentology in Central Europe: New York, Springer-Verlag, p. 106-115.

Bedinger, M. S., F. J. Pearson, Jr., J. E. Reed, R. T. Sniegocki, and C. G. Stone, 1974, The waters of Hot Springs National Park, Arkansas -- their origin, nature, and management: United States Dept. of the Interior, Geol. Survey, 76 p.

Berner, R. A., 1967, Comparative dissolution characteristics of carbonate minerals in the presence and absence of aqueous magnesium ion: Am. Jour. Jour. Sci., v. 265, p. 45-70.

_____, 1971, Principles of chemical sedimentology: New York, McGraw-Hill, 240 p.

Bricker, O. P. (ed.), 1971, Carbonate cements: Baltimore, Johns Hopkins Univ. Studies in Geol., no. 19, 376 p.

Brock, T. D., S. Cook, S. Petersen, and J. L. Mosser, 1976, Biogeochemistry and bacteriology of ferrous iron oxidation in geothermal habitats: Geochim. Cosmochim. Acta, v. 40, p. 493-500.

Broecker, W. S., and V. M. Oversby, 1971, Chemical equilibria in the earth: New York, McGraw-Hill, 318 p.

Brovkov, G. N., 1964, Main features of the diagenesis of the Aalenian coal measures of Dagestan: Intern. Geol. Rev., v. 6, p. 912-919.

Buchbinder, B., Z. B. Begin, and G. M. Friedman, 1974, Pleistocene algal tufa of Lake Lisan, Dead Sea area, Israel: Israel Jour. Earth Sci., v. 23, p. 131-138.

Chave, K. E., 1960, Evidence on the history of sea water from chemistry of deeper subsurface waters of ancient basins: Bull. Am. Assoc. Petrol. Geologists, v. 44, p. 357-370.

Chilingar, G. V., H. J. Bissell, and R. W. Fairbridge (eds.), 1967, Carbonate rocks, Developments in sedimentology, v. 9b: New York, Elsevier, 413 p.

Cosgrove, M. E., 1973, The geochemistry and mineralogy of the Permian red-beds of S.W. England: Chem. Geol., v. 11, p. 31-47.

Cullingford, C. H. D., 1962, British caving: London, Routledge and Kegan Paul Limited, 592 p.

Davies, C. W., and A. L. Jones, 1955, The precipitation of silver chloride from aqueous solutions. 2. Kinetics of growth of seed crystals: Trans. Faraday Soc., v. 51, p. 812-817.

Davis, J. C., 1973, Statistics and data analysis in geology: New York, John Wiley & Sons, 550 p.

Deines, P., D. Langmuir, and R. S. Harmon, 1974, Stable carbon isotype ratios and the existence of a gas phase in the evolution of carbonate ground waters: Geochim. Cosmochim. Acta, v. 38, p. 1147-1164.

Deurer, R., U. Förstner, and G. Schmoll, 1978, Selective chemical extraction of carbonate-associated metals from recent lacustrine sediments: Geochim. Cosmochim. Acta, v. 42, p. 425-427.

Fahraeus, L. E., R. M. Slatt, and G. S. Nowlan, 1974, Origin of carbonate pseudopellets: Jour. Sediment. Petrol., v. 44, p. 27-29.

Faure, G., and P. J. Barrett, 1973, Strontium isotope compositions of non-marine carbonate rocks from the Beacon Supergroup of the Transantarctic Mountains: Jour. Sediment. Petrol., v. 43, p. 447-457.

Folk, R. L., 1974, The natural history of crystalline calcium carbonate: Effect of magnesium content and salinity: Jour. Sediment. Petrol., v. 44, p. 40-53.

_____, and R. Assereto, 1976, Comparative fabrics of length-slow and length-fast calcite and calcitized aragonite in a Holocene speleothem, Carlsbad Caverns, New Mexico: Jour. Sediment. Petrol., v. 46, p. 486-496.

Fournier, R. O., and A. H. Truesdell, 1973, An empirical Na-K-Ca geothermometer for natural waters: Geochim. Cosmochim. Acta, v. 37, p. 1255-1275.

Friedman, G. M., 1968, Geology and geochemistry of reefs, carbonate sediments, and waters, Gulf of Aqaba (Elat), Red Sea: Jour. Sediment. Petrol., v. 38, p. 895-919.

Füchtbauer, H., and H. Goldschmidt, 1964, Aragonitische Lumachellen in bituminösen Wealden des Emslandes: Beitr. Mineral. Petrog., v. 10, p. 184-197.

Fyfe, W. S., and J. L. Bischoff, 1965, The calcite-aragonite problem, in Pray, L. C., and R. C. Murray (eds.), Dolomitization and limestone diagenesis: Soc. Econ. Paleontologists, Spec. Publ., v. 13, p. 3-13.

Garrels, R. M., and C. L. Christ, 1965, Solutions, minerals, and equilibria: New York, Harper & Row, 450 p.

Golubić, S., 1969, Cyclic and noncyclic mechanisms in the formation of travertine: Verh. Int. Verein. Limnol., v. 17, p. 956-961.

Helz, G. R., and S. A. Sinex, 1974, Chemical equilibria in the thermal spring waters of Virginia: Geochim. Cosmochim. Acta, v. 38, p. 1807-1820.

Hem, J. D., 1960, Restraints on dissolved ferrous iron imposed by bicarbonate redox potential, and pH: U. S. Geol. Survey Water-Supply Paper, no. 1459-B, 22 p.

_____, 1972, Chemical factors that influence the availability of iron and manganese in aqueous systems: Bull. Geol. Soc. Am., v. 83, p. 443-450.

_____, and W. H. Cropper, 1959, Survey of ferrous-ferric chemical equilibria and redox potentials: U. S. Geol. Survey Water-Supply Paper, no. 1459-A, 31 p.

Hendy, C. H., 1971, The isotopic geochemistry of speleothems - I. The calculation of the effects of different modes of formation on the isotopic composition of speleothems and their applicability as paleoclimatic indicators: Geochim. Cosmochim. Acta, v. 35, p. 801-824.

Herlinger, D. L., 1977, Travertine deposition, Fall Creek, Idaho: Geol. Soc. Am. Regional Meeting (abstract).

Holland, H. D., M. Borcsik, J. Munoz, and U. M. Oxburgh, 1963, The coprecipitation of Sr^{+2} with aragonite and of Ca^{+2} with strontianite between 90° and 100° C: Geochim. Cosmochim. Acta, v. 27, p. 957-977.

_____, H. J. Holland, and J. L. Munoz, 1964a, The coprecipitation of Sr^{+2} with calcite between 90° and 100° C: Geochim. Cosmochim. Acta, v. 28, p. 1287-1301.

_____, T. V. Kirsipu, J. S. Huebner, and U. M. Oxburgh, 1964b, On some aspects of the chemical evolution of cave waters: Jour. Geol., v. 72, p. 36-67.

Hoskin, C. M., 1968, Magnesium and strontium in mud fraction of recent carbonate sediment, Alacran Reef, Mexico: Bull. Am. Assoc. Petrol. Geologists, v. 52, p. 2170-2177.

Ingerson, E., 1962, Problems of the geochemistry of sedimentary carbonate rocks: Geochim. Cosmochim. Acta, v. 26, p. 815-847.

Irion, G., and G. Müller, 1968a, Huntite, dolomite, magnesite and polyhalite of Recent age from the Tuz Gölü, Turkey: Nature, v. 220, p. 1309-1310.

_____ and _____, 1968b, Mineralogy, petrology and chemical composition of some calcareous tufa from the Schwäbische Alb, Germany, in Müller, G. and G. M. Friedman (eds.), Recent developments in carbonate sedimentology in Central Europe: New York, Springer-Verlag, p. 157-171.

Jacobson, R. L., and D. Langmuir, 1974, Dissociation constants of calcite and $CaHCO_3+$ from 0° to 50° C: Geochim. Cosmochim. Acta, v. 38, p. 301-318.

Kahle, C. F., 1965, Strontium in oölitic limestones: Jour. Sediment. Petrol., v. 35, p. 846-856.

Katy, A., E. Sass, A. Starinsky, and H. D. Holland, 1972, Strontium behavior in the aragonite-calcite transformation: an experimental study at 40°-98° C: Geochim. Cosmochim. Acta, v. 36, p. 481-496.

Kelley, V. C., E. H. Baltz, Jr., and R. A. Bailey, 1961, Road log: Jemez Mountains and vicinity, in Northrop, S. A. (ed.), Guidebook of the Albuquerque County: New Mexico Geol. Soc., no. 12, p. 47-62.

Kinsman, D. J. J., 1966, Coprecipitation of Sr^{+2} with aragonite from sea water at 15°-95° C: Geol. Soc. Am., Spec. Papers, v. 87, p. 88 (abstract).

_____, 1969a, Interpretation of Sr^{+2} concentrations in carbonate minerals and rocks: Jour. Sediment. Petrol., v. 39, p. 486-508.

_____, and H. D. Holland, 1969b, The coprecipitation of cations with $CaCO_3$. IV. The coprecipitation of Sr^{+2} with aragonite between 16° and 96° C: Geochim. Cosmochim. Acta, v. 33, p. 1-17.

Kitano, Y., 1959, State of magnesium in calcium carbonate deposits in thermal springs: Jour. Earth Sci., Nagoya Univ., v. 7, p. 65-79.

_____, 1962, The behavior of various inorganic ions in the separation of calcium carbonate from a bicarbonate solution: Bull. Chem. Soc. Japan, v. 35, p. 1973-1980.

_____ and N. Kawasaki, 1958, Behavior of strontium ion in the process of calcium carbonate separation from bicarbonate solution: Jour. Earth Sci., Nagoya Univ., v. 6, p. 63-74.

Kolesar, P. T., 1968, Mineralogy, geochemistry, and petrography of fresh-water carbonates: Unpub. M.S. thesis, Rennselar Polytechnic Institute, 49 p.

Krauskopf, K. B., 1967, Introduction to geochemistry: New York: McGraw-Hill, 721 p.

Krumbein, W. C., and F. A. Graybill, 1965, An introduction to statistical models in geology: New York, McGraw-Hill, 475 p.

Kübler, B., 1962, Étude pétrographique de L'Oehningien (Tortonien) du Locle (Suisse occidentale): Beitr. Mineral. Petrog., v. 8, p. 267-314

Kulp, J. L., K. K. Turekian, and D. W. Boyd, 1952, Strontium content of limestones and fossils: Bull. Geol. Soc. Am., v. 63, p. 710-716.

Lafon, G. M., 1970, Calcium complexing with carbonate ion in aqueous solutions at 25° C and 1 atm.: Geochim. Cosmochim. Acta, v. 34, p. 935-940.

Langmuir, D., 1971, The geochemistry of some carbonate ground waters in central Pennsylvania: Geochim. Cosmochim. Acta, v. 35, p. 1023-1045.

Latimer, W. M., 1952, The oxidation states of the elements and their potentials in aqueous solutions: New York, Prentice-Hall, 392 p.

Lattman, L. H., and E. M. Simonberg, 1971, Case-hardening of carbonate alluvium and colluvium, Spring Mountains, Nevada: Jour. Sediment. Petrol., v. 41, p. 274-281.

Lindholm, R. C., and R. B. Finkleman, 1972, Calcite staining: semi-quantitative determination of ferrous iron: Jour. Sediment. Petrol., v. 42, p. 239-242.

_____, and D. A. Dean, 1973, Ultra-thin thin sections in carbonate petrology: a valuable tool: Jour. Sediment. Petrol., v. 43, p. 295-297.

Lippmann, F., 1960, Versuche zur Aufklärung der Bildungsbedingungen von Kalzit und Aragonit: Fortschr. Mineral., v. 38, p. 156-161.

_____, 1973, Sedimentary carbonate minerals: New York, Springer-Verlag, 228 p.

Matthews, R. K., 1966, Genesis of recent lime mud in southern British Honduras: Jour. Sediment. Petrol., v. 36, p. 428-454.

_____, 1967, Diagenetic fabrics in biosparites from the Pleistocene of Barbados, West Indies: Jour. Sediment. Petrol., v. 37, p. 1147-1153.

Miller, R. L., and J. S. Kahn, 1962, Statistical analysis in the geological sciences: New York, John Wiley & Sons, 283 p.

Milliman, J. D., and B. Bornhold, 1973, Discussion: peak height versus peak intensity analysis of X-ray diffraction data: Sedimentology, v. 20, p. 445-448.

Mitterer, R. M., 1971, Influence of natural organic matter on $CaCO_3$ precipitation, in Bricker, O. P. (ed.), Carbonate cements: Baltimore, Johns Hopkins Univ. Studies in Geol., p. 252-258.

Moberly, R., 1973, Rapid chamber-filling growth of marine aragonite and Mg-calcite: Jour. Sediment. Petrol., v. 43, p. 634-635.

Möller, P., and H. Papendorf, 1971, Fractionation of calcium isotypes in carbonate precipitates: Earth Planet. Sci. Lett., v. 11, p. 192-194.

Molnia, B. F., 1974, A rapid and accurate method for the analysis of calcium carbonate in small samples: Jour. Sediment. Petrol., v. 44, p. 589-590.

Moorhouse, W. W., 1959, The study of rocks in thin sections: New York, Harper & Row, 514 p.

Müller, G., 1962, Zur geochemie des strontiums in ozeanen evaporiten unter besonderer Berücksichtigung der sedimentären Coelestinlagerstätte Von Hemmelte - West (Süd-Oldenburg): Beih. Geol. Jahrb., v. 35, 90 p.

_____, 1968, Exceptionally high strontium concentrations in fresh water onkolites and mollusk shells of Lake Constance, in Müller, G., and G. M. Friedman (eds.), Recent developments in carbonate sedimentology in Central Europe: New York, Springer-Verlag, 255 p.

_____, 1969a, High strontium contents and Sr/Ca- ratios in Lake Constance waters and carbonates and their sources in the drainage area of the Rhine river (Alpenrhein): Mineral. Deposita, v. 4, p. 75-84.

_____, 1969b, Diagenetic changes in interstitial waters of Holocene Lake Constance sediments: Nature, v. 224, p. 258-259.

_____, 1971, Sediments of Lake Constance, in Müller, G. (ed.), Sedimentology of parts of Central Europe: Frankfurt, Kramer, p. 237-252.

_____, and G. M. Friedman (eds.), 1968, Recent developments in carbonate sedimentology in Central Europe: New York, Springer-Verlag, 255 p.

_____, G. Irion, and U. Förstner, 1972, Formation and diagenesis of inorganic Ca-Mg carbonates in the lacustrine environment: Naturwissenschaften, v. 59, p. 158-164.

Murray, J. W., 1954, The deposition of calcite and aragonite in caves: Jour. Geol., v. 62, p. 481-492.

Odum, H. T., 1957, Biochemical deposition of strontium: Inst. Marine Sci. Publ., v. 4, p. 38-114.

Oxburgh, U. M., R. E. Segnit, and H. D. Holland, 1959, Coprecipitation of strontium with calcium carbonate from aqueous solutions: Program Geol. Soc. Am. Meeting -- Pittsburgh, 95A-96A.

Paterson, K., 1972, Responses in the chemistry of spring waters in the Oxford region to some climatic variables: Trans. Cave Res., Group G. B., v. 14, p. 132-140.

Peterson, M. N. A., G. S. Bien, and R. A. Berner, 1963, Radiocarbon studies of recent dolomite from Deep Spring Lake, California: Jour. Geophys. Res., v. 68, p. 6493-6505.

Pitty, A. F., 1971, Rate of uptake of calcium carbonate in underground karst water: Geol. Mag., v. 108, p. 537-543.

Purdy, E. G., 1974, Karst-determined facies patterns in British Honduras: Holocene carbonate sedimentation model: Bull. Am. Assoc. Petrol. Geologists, v. 58, p. 825-855.

Read, J. F., 1974, Calcrete deposits and Quaternary sediments, Edel Province, Western Australia: Memoir Am. Assoc. Petrol. Geologists, no. 22, p. 250-282.

Rösler, H. J., and H. Lange, 1972, Geochemical tables: New York, Elsevier, 468 p.

Runnells, D. D., 1969, Diagenesis, chemical sediments, and the mixing of natural waters: Jour. Sediment. Petrol., v. 39, p. 1188-1201.

_____, 1970, Errors in X-ray analysis of carbonates due to solid solution variation in composition of component minerals: Jour. Sediment. Petrol., v. 40, p. 1158-1166.

Salomons, W., 1975, Chemical and isotopic composition of carbonates in Recent sediments and soils from Western Europe: Jour. Sediment. Petrol., v. 45, p. 440-449.

Scholle, P. A., 1978, Carbonate rock constituents, textures, cements, and porosities: Am. Assoc. Petrol. Geologists, Memoir 27, 241 p.

_____, and D. J. J. Kinsman, 1974, Aragonitic and high-Mg calcite caliche from the Persian Gulf -- a modern analog for the Permian of Texas and New Mexico: Jour. Sediment. Petrol., v. 44, p. 904-916.

Shapiro, L., 1975, Rapid analysis of silicate, carbonate, and phosphate rocks -- revised edition: Bull. U. S. Geol. Survey, no. 1401, 76 p.

Shcherbina, V. V., 1975, Geochemistry of elements of medium abundance, in Tugarinov, A. I. (ed.), Recent contributions to geochemistry and analytical chemistry: New York, John Wiley & Sons, p. 312-317.

Siebold, E., 1962, Kalk-Konkretionene und karbonatisch gebundenes magnesium: Geochim. Cosmochim. Acta, v. 26, p. 899-909.

Siegel, F. R., 1960, The effect of strontium on the aragonite-calcite ratios of Pleistocene corals: Jour. Sediment. Petrol., v. 30, p. 297-304.

_____, 1961, Variations of Sr/Ca ratios and Mg contents in recent carbonate sediments of the Northern Florida Keys area: Jour. Sediment. Petrol., v. 31, p. 336-342.

_____, and M. W. Reams, 1966, Temperature effect on precipitation of calcium carbonate from calcium bicarbonate solutions and its application to cavern environments: Sedimentology, v. 7, p. 241-248.

Sippel, R. F., and E. D. Glover, 1965, Structures in carbonate rocks made visible by luminescence petrography: Science, v. 150, p. 1283-1287.

Skinner, H. C. W., 1963, Precipitation of calcian dolomites and magnesian calcites in the southeast of South Australia: Am. Jour. Sci., v. 261, p. 449-472.

Skougstad, M. W., and C. A. Horr, 1963, Occurrence and distribution of strontium in natural water: U. S. Geol. Survey, Water Supply Paper, no. 1496-D, p. 55-97.

Smith, H. M., 1970, Identification of organic matter in thin section by staining and a study programme for carbonate rocks: Jour. Sediment. Petrol., v. 40, p. 1350-1351.

Sommer, S. E., 1972, Cathodoluminescence of carbonates. 1. Characterization of cathodoluminescence from carbonate solid solutions: Chem. Geol., v. 9, p. 257-273.

Stehli, F. G., and J. Hower, 1961, Mineralogy and early diagenesis of carbonate sediments: Jour. Sediment. Petrol., v. 31, p. 358-371.

Suess, E., 1973, Interaction of organic compounds with calcium carbonate -- II: Geochim. Cosmochim. Acta, v. 37, p. 2435-2448.

Taft, W. H., and J. W. Harbaugh, 1964, Modern carbonate sediments of southern Florida, Bahamas, and Espíritu Santo Island, Baja California: a comparison of their mineralogy and chemistry: Stanford Univ. Publ., Univ. Ser., Geol. Sci., v. 8, p. 1-133.

Terlecky, M. P. Jr., 1974, The origin of a Late Pleistocene and Holocene marl deposit: Jour. Sediment. Petrol., v. 44, p. 456-465.

Thompson, T. G., and T. J. Chow, 1955, The strontium-calcium atom ratio in carbonate-secreting marine organisms: Deep-Sea Res., Suppl., v. 3, p. 20-39.

Thrailkill, J., 1971, Carbonate deposition in Carlsbad Caverns: Jour. Geol., v. 79, p. 683-695.

Trainer, F. W., 1975, Mixing of thermal and nonthermal waters in the margin of the Rio Grande Rift, Jemez Mountains, New Mexico, in Seager, W. R., R. E. Clemons, and J. F. Callender (eds.), Guidebook of the Las Cruces County: New Mexico Geol. Soc., no. 26, p. 213-218.

Turekian, K. K., and L. Armstrong, 1964, Magnesium, strontium, and barium concentrations and calcite-aragonite ratios of some recent molluscan shells: Jour. Marine Res. (Sears Foundation), v. 18, p. 198-215.

_____, and J. L. Kulp, 1956, The geochemistry of strontium: Geochim. Cosmochim. Acta, v. 10, p. 245-296.

Usdowski, H. E., 1963, Die Genese der Turenmergel oder Nagelkalke (cone-in-cone): Beitr. Mineral. Petrog., v. 9, p. 95-110.

_____, 1964, Dolomit im system Ca^{+2}-Mg^{+2}-CO_3^{+2}-Cl_2^{2-}-H_2O: Naturwissenschaften, v. 51, p. 357.

Veizer, J., and R. Demovic, 1974, Strontium as a tool in facies analysis: Jour. Sediment. Petrol., v. 44, p. 93-115.

_____, _____, and J. Turan, 1971, Possible use of strontium in sedimentary carbonate rocks as a paleo-environmental indicator: Sediment. Geol., v. 5, p. 5-22.

Vinogradov, A. P., and A. B. Ronov, 1956, Composition of the sedimentary rocks of the Russian platform in relation to the history of its tectonic movements: Geochem., v. 6, p. 533-559.

Walter, M. R., (ed.), 1976, Stromatolites, Developments in sedimentology, v. 20: New York, Elsevier, 790 p.

Weber, J. N., 1964, Trace element composition of dolostones and dolomites and its bearing on the dolomite problem: Geochim. Cosmochim. Acta, v. 28, p. 1817-1868.

_____, 1968, Quantitative mineralogical analysis of carbonate sediments: comparison of X-ray diffraction and electron probe microanalyser methods: Jour. Sediment. Petrol., v. 38, p. 232-234.

Whelen, T., and H. H. Roberts, 1973, Carbon isotope composition of diagenetic carbonate nodules from freshwater swamp environments: Jour. Sediment. Petrol., v. 43, p. 54-58.

White, D. E., 1957, Thermal waters of volcanic origin: Bull. Geol. Soc. Am., v. 68, p. 1637-1658.

Whitehead, D., 1976, The determination of calcium and magnesium in carbonate rocks by atomic-absorption spectrophotometry after acid decomposition: Chem. Geol., v. 18, p. 149-154.

Wilkniss, P. E., T. B. Warner, and R. A. Carr, 1971, Some aspects of the geochemistry of F, Fe, and Mn in coastal waters and in freshwater springs on the southeast coast of Hawaii: Marine Geol., v. 11, p. M39-M46.

Wilson, J. L., 1975, Carbonate facies in geologic history: New York, Springer-Verlag, 471 p.

Zeller, E. J., and J. L. Wray, 1956, Factors influencing precipitation of calcium carbonate: Bull. Am. Assoc. Petrol. Geologists, v. 40, p. 140-152.

APPENDIXES

APPENDIX A

MODAL ANALYSES OF SELECTED TRAVERTINE SAMPLES

Sample No.	TMQI-B	TMQI-126	TMQI-166	TMQI-188
Allochemical Components				
quartz	3.0	tr	tr	2.0
feldspar	1.0	tr	tr	2.0
sulfides	tr	tr	tr	tr
magnetite	1.0	tr	tr	1.0
hematite$_{(xl)}$	tr	-	-	tr
apatite	1.0	tr	1.0	tr
rock fragments	-	-	-	-
collophane?	tr	-	tr	-
other (trace)	musco-vite	-	-	-
Orthochemical Components				
micrite	10.0	20.0	85.0	50.0
sparite	36.0	19.0	8.0	6.9
spar	10.0	3.0	1.0	5.0
aragonite	-	-	-	-
clay	12.0	2.0	tr	3.0
hematite$_{(ox)}$	10.0	-	-	tr
chalcedony	-	tr	-	-
Voids	15.0	55.0	4.0	30.0
Organic Remains	-	-	-	-

Sample No.	TMQII-150	TMQII-288	SP-I	SP-II
Allochemical Components				
quartz	54	1.0	54	tr
feldspar	tr	1.0	tr	tr
sulfides	tr	tr	tr	tr
magnetite	1.0	tr	tr	tr
hematite$_{(xl)}$	tr	tr	1.0	1.0
apatite	tr	tr	tr	tr
rock fragments	-	1.0	-	-
collophane?	-	tr	-	tr
other (trace)	-	bio-tite	-	-
Orthochemical Components				
micrite	75.0	30.0	10.0	40.0
sparite	8.0	30.0	46.0	10.0
spar	7.0	2.0	16.0	3.0
aragonite	-	-	4.0	-
clay	tr	tr	1.0	tr
hematite$_{(ox)}$	tr	tr	9.0	3.0
chalcedony	tr	-	tr	-
Voids	8.0	34.0	12.0	42.0
Organic Remains	-	-	-	-

Sample No.	SP-III	A	B	D	M1
Allochemical Components					
quartz	2.0	-	tr	tr	-
feldspar	2.0	-	7.0	1.0	-
sulfides	tr	tr	tr	tr	tr
magnetite	tr	2.0	5.0	2.0	tr
hematite$_{(xl)}$	tr	tr	-	tr	-
apatite	tr	-	-	tr	-
rock fragments	2.0	-	12.0	2.0	-
collophane?	tr	tr	-	-	-
other (trace)	-	-	-	musco-vite	-
Orthochemical Components					
micrite	50.0	20.0	10.0	10.0	5.0
sparite	8.0	45.0	32.0	30.0	38.0
spar	1.0	26.0	24.0	28.0	15.0
aragonite	tr	-	-	-	-
clay	tr	1.0	3.0	10.0	11.0
hematite$_{(ox)}$	tr	1.0	3.0	1.0	tr
chalcedony	tr	tr	tr	-	tr
Voids	34.0	4.0	3.0	15.0	30.0
Organic Remains	-	-	-	-	-

APPENDIX B

X-RAY DIFFRACTION ANALYSES FOR MAGNESIUM CONTENT IN SELECTED FRESHWATER CARBONATES

Sample No.	(112) Reflection 2θ (Degrees)	Mol % Mg
B3TOM	29.70	9.0
B3EOD	29.55	4.0
FC10	29.65	7.0
FC12	29.58	5.0
SPI	30.10	22.0
SPIII	29.58	5.0
QI126	29.78	12.0
QI150	29.59	6.0
QI166	29.55	4.0
QI216	29.88	14.0
QII126	29.83	13.0
QII186	29.55	4.0
QII222	29.55	4.0
QII288	29.55	4.0
QFISSM	29.70	9.0

Sample No.	(112) Reflection 2θ (Degrees)	Mol % Mg
GI30FS	30.38	30.0
GII20R	30.37	29.0
A	29.55	4.0
B	30.22	27.0
D	29.70	9.0
M1	29.71	10.0
M3	29.59	6.0
K-12	29.55	4.0
K-13	29.55	4.0
ND2A	29.55	4.0
ND2B	29.59	6.0
PITE2	29.58	5.0
CB8	29.58	5.0
VMD	29.58	5.0
NLBL	29.70	9.0

APPENDIX C

CHEMICAL ANALYSES OF FRESHWATER CARBONATES

GEOCHEMICAL ANALYSIS OF FRESHWATER CARBONATES ----- ELEMENTAL CONCENTRATIONS IN PPM, RESIDUE WEIGHT IN GM/FRACTION

LOC=CB

OBS	LOC	SAMPID	SAMPLET	RESID	CA	MG	FE	MN	SR	NA	K	LI	BA	ZN	PB	CU	NI	CR	TOTAL	MGCARAT	SRCARAT	MNFERAT
1	CB	CB3	A	0.5890	207000	2567	1415	219	110	2859	766	3	122	11	60	24	14	12	215182	2.0446	0.24306	15.733
2	CB	CB4	B	0.2118	358000	2411	411	476	165	920	235	3	0	5	63	13	15	6	362723	1.1103	0.21083	117.733
3	CB	CB5	C	0.1918	159000	77000	3624	767	1732	1701	699	6	617	17	50	19	9	6	245247	79.8429	4.98282	21.515
4	CB	CB6	D	0.5014	268000	15323	1920	1033	913	2878	612	7	400	21	30	30	30	10	291207	9.4265	1.55833	54.693
5	CB	CB7	E	0.5356	291000	16419	2207	1163	958	2767	506	10	217	45	34	22	12	11	315371	9.3024	1.50590	53.569
6	CB	CB8	F	0.0528	322000	1742	379	222	106	998	206	1	105	8	41	16	0	5	325829	0.8919	0.15058	59.545
7	CB	CB9	G	0.1234	402000	2681	534	359	108	759	200	2	739	14	45	131	13	6	407591	1.0995	0.12289	68.342
8	CB	CB10	H	0.1857	467000	4710	414	289	190	663	147	3	741	19	40	37	15	6	474274	1.6629	0.18611	70.963
9	CB	CB11	I	0.0960	380000	2157	572	409	100	680	127	3	167	13	33	278	7	5	384551	0.9359	0.12038	72.688
10	CB	CB12	J	0.0240	294000	2418	1000	210	113	763	328	2	408	18	44	20	16	5	299345	1.3560	0.17581	21.348

LOC=FC

OBS	LOC	SAMPID	SAMPLET	RESID	CA	MG	FE	MN	SR	NA	K	LI	BA	ZN	PB	CU	NI	CR	TOTAL	MGCARAT	SRCARAT	MNFERAT
11	FC	FC3SPT	A	0.1088	298000	4129	2865	185	258	477	90	2	112	22	34	28	18	6	306226	2.2844	0.39603	6.564
12	FC	B2TOM	B	0.0197	343000	4791	995	2142	352	413	168	2	306	29	35	26	36	5	352300	2.3029	0.46943	218.842
13	FC	B3FOD	C	0.4353	276000	11378	9973	204	390	841	2568	8	268	323	54	36	17	9	302069	6.7967	0.64637	2.079
14	FC	B3TOR	D	0.3074	232000	2238	52536	6136	173	1075	426	1	870	29	30	36	12	3	295562	1.5904	0.34110	11.873
15	FC	B3TOM	E	0.0157	343000	3962	3286	442	361	442	183	0	102	7	50	26	16	5	351882	1.9044	0.48143	13.674
16	FC	FC10	F	0.5212	258000	18100	7500	512	1180	898	1556	13	625	55	52	52	0	10	288553	11.5665	2.09212	6.940
17	FC	FC11	G	0.6162	248000	13874	28026	521	691	938	1355	9	263	57	47	66	16	13	293876	9.2234	1.27453	1.890
18	FC	FC12	H	0.5812	283000	13500	11667	513	1146	895	1218	12	357	57	60	48	38	12	312523	7.8648	1.85235	4.470

LOC=GU

OBS	LOC	SAMPID	SAMPLET	RESID	CA	MG	FE	MN	SR	NA	K	LI	BA	ZN	PB	CU	NI	CR	TOTAL	MGCARAT	SRCARAT	MNFERAT
19	GU	GII20R	A	0.0484	322000	6295	9105	431	4098	1534	494	13	158	28	32	16	1	5	344210	3.2232	5.8216	4.8121
20	GU	GII0M	B	0.6764	50700	15204	102344	1283	3090	3523	4944	16	156	166	76	63	42	31	181638	49.4416	27.8789	1.2744
21	GU	GI0M	C	0.2825	251000	2216	105000	181	1254	2369	1199	6	764	76	125	42	28	14	364274	1.4556	2.2853	0.1752
22	GU	GISPT	D	0.0064	315000	7317	586	403	3925	1223	86	18	101	36	36	20	0	3	328754	3.8297	5.6997	69.9104
23	GU	GISST	E	0.0348	359000	6082	3742	440	4610	1642	378	16	206	26	34	26	0	0	376202	2.7932	5.8740	11.9532
24	GU	GI8FS	F	0.0442	331000	5493	20417	539	4499	973	387	16	104	50	36	21	6	5	363546	2.7361	6.2175	2.6837
25	GU	GI30FS	G	0.0484	316000	7619	4263	289	7514	1708	441	22	153	27	39	21	16	5	338117	3.9752	10.8770	6.8916
26	GU	GI3FS	H	0.0974	360000	6742	27677	670	5540	1762	1568	43	167	72	37	22	12	6	404318	3.0877	7.0393	2.4609
27	GU	GI20WM	I	0.0029	354000	7475	990	125	4500	1180	90	13	150	21	35	25	10	5	368619	3.4814	5.8148	12.8354
28	GU	GI25R	J	0.0481	347000	6986	4711	378	5778	1523	368	17	158	27	35	21	6	5	367013	3.3193	7.6168	8.1567
29	GU	GI40ST	K	0.0811	320000	19000	4457	234	8597	1507	452	32	0	29	49	16	17	6	354396	9.7892	12.2891	5.3371
30	GU	GI45FS	L	0.0070	321000	12800	1061	186	4935	1385	201	13	101	22	41	20	20	7	341792	6.5743	7.0324	17.8210

GEOCHEMICAL ANALYSIS OF FRESHWATER CARBONATES ----- ELEMENTAL CONCENTRATIONS IN PPM, RESIDUE WEIGHT IN GM/FRACTION

LOC=K-

OBS	LOC	SAMPID	SAMPLET	RESID	CA	MG	FE	MN	SR	NA	K	LI	BA	ZN	PB	CU	NI	CR	TOTAL	MGCARAT	SRCARAT	MNFERAT
31	K-	1	A	0.1549	232000	1248	512	379	160	408	166	2	118	8	34	18	2	6	235061	3.88689	0.315469	75.250
32	K-	2	B	0.3032	290000	1981	3279	660	244	545	1134	2	0	6	36	14	1	7	297909	1.12624	0.384872	20.461
33	K-	5	C	0.1193	262000	2294	1119	1760	170	295	261	2	0	6	45	17	7	6	267982	1.44356	0.296806	159.888
34	K-	6	D	0.1818	288000	1522	970	2078	183	312	244	1	244	7	42	18	8	6	293635	0.87129	0.290659	217.775
35	K-	7	E	0.2582	320000	10178	3703	1550	317	202	378	2	135	8	46	20	4	7	336550	5.24391	0.453141	42.551
36	K-	8	F	0.2885	398000	2741	803	829	295	640	239	1	0	7	56	21	18	7	403657	1.13545	0.339050	104.948
37	K-	9	G	0.1615	288000	6679	2333	1789	286	251	209	3	0	17	51	18	0	0	299636	3.82351	0.454253	77.953
38	K-	10	H	0.4311	309000	1688	1149	1846	273	1072	554	1	175	9	53	26	8	6	315860	0.90065	0.404137	163.323
39	K-	11	I	0.1171	269000	1246	750	2095	170	561	210	1	0	9	49	11	13	6	274121	0.76367	0.289082	283.960
40	K-	12	J	0.5618	270000	1198	1216	1267	308	285	571	1	0	14	52	23	0	0	274935	0.73154	0.521809	105.920
41	K-	13	K	0.4030	284000	1524	1175	1566	310	0	444	1	167	13	42	25	7	6	289280	0.88473	0.499307	135.484
42	K-	14	L	0.1454	298000	1861	829	2282	246	568	222	1	118	9	53	18	0	0	304207	1.02961	0.377610	279.831
43	K-	15	M	0.3945	306000	1866	1385	2477	173	273	372	1	0	11	51	16	15	8	312648	1.00539	0.258612	181.807

LOC=M-

OBS	LOC	SAMPID	SAMPLET	RESID	CA	MG	FE	MN	SR	NA	K	LI	BA	ZN	PB	CU	NI	CR	TOTAL	MGCARAT	SRCARAT	MNFERAT
44	M-	M	A	0.0178	300000	1873	1031	957	255	723	158	11	153	16	51	26	31	5	305290	1.02934	0.388815	94.3600
45	M-	M1	B	0.0372	313000	3635	1745	73	270	597	280	13	625	22	31	26	27	5	320349	1.91471	0.394588	4.2527
46	M-	M2	C	0.0156	306000	2819	949	36	127	574	290	11	408	87	36	26	21	5	311389	1.51886	0.189848	3.8563
47	M-	M3	D	0.0321	340000	4546	526	26	315	548	119	12	516	27	35	26	18	5	346719	2.20441	0.423795	5.0248

LOC=ND

OBS	LOC	SAMPID	SAMPLET	RESID	CA	MG	FE	MN	SR	NA	K	LI	BA	ZN	PB	CU	NI	CR	TOTAL	MGCARAT	SRCARAT	MNFERAT
48	ND	2A	A	0.1413	268000	2416	2209	1630	309	349	291	1	0	12	35	23	99	215	275589	1.48629	0.52741	75.0113
49	ND	2B	B	0.5135	295000	3813	15000	2878	648	421	442	2	204	19	51	143	5	41	318667	2.13102	1.00479	19.5045
50	ND	VMD	C	0.4879	243000	1758	9608	7713	234	449	342	2	98	67	39	59	99	438	263906	1.19277	0.44049	81.6065
51	ND	NLBL	D	0.2627	335000	2679	3378	2848	271	312	217	2	135	14	35	34	14	34	344973	1.31847	0.37004	85.7067
52	ND	4	E	0.6636	222000	5039	58824	2361	223	669	639	4	0	103	36	44	88	29	290059	3.74226	0.45949	4.0801

LOC=SD

OBS	LOC	SAMPID	SAMPLET	RESID	CA	MG	FE	MN	SR	NA	K	LI	BA	ZN	PB	CU	NI	CR	TOTAL	MGCARAT	SRCARAT	MNFERAT
53	SD	A	A	0.0033	342000	1810	765	1550	110	295	45	9	0	13	35	15	0	5	346652	0.87256	0.147127	205.970
54	SD	B	B	0.0733	310000	2590	479	1673	259	416	194	13	591	10	40	16	20	5	316306	1.37747	0.382175	355.054
55	SD	C	C	0.0131	327000	3775	293	10	147	659	142	16	303	111	30	25	0	7	332518	1.90332	0.205634	3.470
56	SD	D	D	0.0353	337000	4302	693	762	726	674	259	19	781	6	42	16	27	5	345312	2.10467	0.985442	111.778
57	SD	E	E	0.0092	333000	1448	535	1413	262	520	20	6	253	15	46	51	25	5	337599	0.71691	0.359900	268.487
58	SD	F	F	0.0508	316000	1633	474	1038	269	306	47	6	316	5	42	37	53	6	320232	0.85200	0.389394	222.615

GEOCHEMICAL ANALYSIS OF FRESHWATER CARBONATES ----- ELEMENTAL CONCENTRATIONS IN PPM, RESIDUE WEIGHT IN GM/FRACTION

LOC=ST

OBS	LOC	SAMPID	SAMPLET	RESID	CA	MG	FE	MN	SR	NA	K	LI	BA	ZN	PB	CU	NI	CR	TOTAL	MGCARAT	SRCARAT	MNFERAT
59	ST	A2	A	0.1818	295000	2561	1707	1589	141	0	709	1	183	20	37	24	39	10	302021	1.43130	0.218636	94.629
60	ST	A4	B	0.0373	276000	1428	365	1870	109	0	57	1	104	10	50	16	21	8	280039	0.85303	0.180652	520.815
61	ST	A5	C	0.3926	288000	2610	1508	1498	165	165	486	2	3	18	49	25	39	9	294574	1.49414	0.262069	100.982
62	ST	PITE2	D	0.1284	285000	2226	356	511	184	0	178	1	58	10	46	17	30	6	288623	1.28772	0.295323	145.917

LOC=TM

OBS	LOC	SAMPID	SAMPLET	RESID	CA	MG	FE	MN	SR	NA	K	LI	BA	ZN	PB	CU	NI	CR	TOTAL	MGCARAT	SRCARAT	MNFERAT
63	TM	QII8	A	0.1129	145000	2198	2332	68	56	271	180	0	0	62	11	28	57	152	150415	2.4992	0.176663	2.9643
64	TM	QII24	B	0.1296	400000	7778	1069	109	149	253	144	3	0	81	34	29	2	6	409657	3.2059	0.170393	10.3653
65	TM	QII48	C	0.1359	335000	5266	6744	324	133	162	145	2	116	132	47	64	7	9	348151	2.5917	0.191606	4.8838
66	TM	QII72	D	0.0234	253000	8166	1148	56	118	256	287	6	51	122	42	41	0	26	263319	5.3215	0.213347	4.9588
67	TM	QII98	E	0.1112	344000	3657	1332	90	141	242	96	3	112	85	34	28	1	6	349827	1.7527	0.187493	6.8687
68	TM	QII102	F	0.0168	343000	5925	1010	534	163	224	122	3	102	143	40	77	21	56	351420	2.8480	0.217379	53.7470
69	TM	QII126	G	0.0481	316000	5804	1247	152	147	368	116	3	158	118	36	53	11	5	324218	3.0282	0.212792	12.3912
70	TM	QII150	H	0.0134	345000	4080	1273	1034	127	390	66	3	253	172	40	96	25	35	352594	1.9498	0.168387	82.5708
71	TM	QII186	I	0.1028	307000	6186	3545	947	190	312	368	3	278	143	31	67	7	233	319310	3.3221	0.283100	27.1562
72	TM	QII222	J	0.0993	295000	8638	1089	100	150	555	305	4	167	142	38	33	7	11	306239	4.8276	0.232591	9.3348
73	TM	QII288	K	0.0579	345000	5106	1702	80	228	297	292	2	106	76	32	21	10	5	352957	2.4401	0.302301	4.7782
74	TM	QIIUN	L	0.0758	307000	6817	1147	43	114	184	216	4	0	138	43	22	13	8	315749	3.6610	0.169860	3.8110
75	TM	QI8	M	0.0658	361000	4630	2086	177	182	278	203	2	161	153	27	43	49	91	369082	2.1145	0.230616	8.6257
76	TM	QI30	N	0.0288	359000	3321	722	67	129	324	98	1	0	175	30	31	11	16	363875	1.5252	0.164369	9.4335
77	TM	QI48	O	0.2046	227000	4067	2006	38	107	402	245	1	125	90	34	38	9	6	234168	2.9539	0.215617	1.9257
78	TM	QI72	P	0.3834	216000	5433	1710	219	89	495	422	3	161	111	32	57	47	0	224779	4.1469	0.188478	13.0191
79	TM	QI96	Q	0.0455	341000	4023	2042	121	141	278	100	2	211	133	38	37	95	5	348226	1.9451	0.189143	6.0237
80	TM	QI126	R	0.0004	324000	4310	1535	30	245	300	25	2	250	88	29	25	85	185	331109	2.1932	0.345896	1.9868
81	TM	QI150	S	0.1336	318000	12800	2167	110	185	266	421	4	172	79	31	29	99	253	334616	6.6363	0.266115	5.1602
82	TM	QI166	T	0.0034	265000	4940	250	15	150	0	20	2	100	71	36	15	15	5	270619	3.0734	0.258923	6.0994
83	TM	QI188	U	0.0771	333000	8018	1717	813	255	363	271	6	435	142	40	54	17	5	345136	3.9698	0.350284	48.1343
84	TM	QI216	V	0.0434	364000	8164	2292	146	403	518	314	4	208	42	36	31	63	143	376364	3.6978	0.506440	6.4755
85	TM	QSPIA	W	0.0154	343000	5078	245	5	254	498	66	2	204	76	36	26	31	40	349551	2.4409	0.338738	2.0746
86	TM	QFISSM	X	0.0147	351000	4060	505	10	208	406	56	2	202	187	36	25	25	35	356757	1.9070	0.271070	2.0130
87	TM	QSPI	Y	0.0129	360000	3000	2200	1116	595	516	60	4	210	135	39	30	60	120	368085	1.3739	0.756030	51.5675
88	TM	QSPIII	Z	0.1100	350000	23000	1438	129	270	348	332	18	225	96	39	28	41	68	376032	10.8343	0.352874	9.1194

Key:

CB = Corbin Paleosoil
FC = Kelly Ranch Travertine
GU = Guffy Travertine
K- = Devonian Cornstones
M- = Verde Fm. Lake Carbonate
ND = Post Oak Paleosoil
SD = Soda Dam Travertine
ST = Scottish Paleosoil
TM = Twin Mountains Travertine

APPENDIX D

CORRELATION MATRICES AND FACTOR PATTERNS FOR TWIN MOUNTAINS, GUFFY, KELLY RANCH, AND SODA DAM

TWIN MOUNTAINS

Correlation Matrix

	Resid	Ca	Mg	Fe	Mn	Sr
Resid	1.00000	-0.22159	0.25616	0.45011	0.27936	-0.35353
Ca	-0.22159	1.00000	0.28399	-0.09360	0.16517	0.66730
Mg	0.25616	0.28399	1.00000	0.03602	0.08150	0.25946
Fe	0.45011	-0.09360	0.03602	1.00000	0.65415	-0.02341
Mn	0.27936	0.16517	0.08150	0.65415	1.00000	0.15849
Sr	-0.35353	0.66730	0.25946	-0.02341	0.15849	1.00000

Varimax Factor Pattern

Factors	1	2	3	4	5	6
Eigenvalues	2.013481	1.927319	1.046505	0.427694	0.339609	0.245392
Portion	0.336	0.321	0.174	0.071	0.057	0.041
Cum. Portion	0.336	0.657	0.831	0.902	0.959	1.000

	Factor 1	Factor 2	Factor 3	Factor 4	Factor 5
Resid	0.19469	-0.17942	0.16971	0.93945	0.06068
Ca	0.07367	0.94660	0.11001	-0.03702	-0.19611
Mg	0.01864	0.17584	0.97127	0.14167	0.00561
Fe	0.71036	-0.08296	-0.03392	0.33977	0.55016
Mn	0.97319	0.13049	0.04165	0.08417	-0.01914
Sr	0.04102	0.80189	0.18801	-0.34149	0.37069

GUFFY

Correlation Matrix

	Resid	Ca	Mg	Fe	Mn	Sr
Resid	1.00000	-0.61492	-0.97989	0.91947	0.57140	-0.32524
Ca	-0.61492	1.00000	-0.31824	-0.55467	-0.57222	0.35181
Mg	-0.07989	-0.31824	1.00000	-0.30363	0.18404	0.65596
Fe	0.91947	-0.55467	-0.30363	1.00000	0.50401	-0.51492
Mn	0.57140	-0.57222	0.18404	0.50401	1.00000	0.01740
Sr	-0.32524	0.35181	0.65596	-0.51492	0.01740	1.00000

Varimax Factor Pattern

Factors	1	2	3	4	5	6
Eigenvalues	3.081868	1.764547	0.636842	0.417497	0.050247	0.048999
Portion	0.514	0.294	0.106	0.070	0.008	0.008
Cum. Portion	0.514	0.808	0.914	0.983	0.992	1.000

	Factor 1	Factor 2	Factor 3	Factor 4	Factor 5
Resid	0.92213	-0.07554	-0.25118	-0.24289	-0.10881
Ca	-0.36690	-0.02190	0.87890	0.28547	-0.01337
Mg	-0.12618	0.90199	-0.38517	-0.94759	0.11242
Fe	0.88786	-0.31146	-0.18041	-0.23189	0.14418
Mn	0.32383	0.10367	-0.22057	-0.91356	0.00068
Sr	-0.20524	0.88201	0.37567	-0.08662	-0.13821

KELLY RANCH

Correlation Matrix

	Resid	Ca	Mg	Fe	Mn	Sr
Resid	1.00000	-0.86238	0.60787	0.76347	-0.13514	0.46004
Ca	-0.86238	1.00000	-0.22686	-0.90958	-0.23436	-0.10186
Mg	0.60787	-0.22686	1.00000	0.12423	-0.51264	0.90859
Fe	0.76347	-0.90958	0.12423	1.00000	0.26191	0.04611
Mn	-0.13514	-0.23436	-0.51264	0.26191	1.00000	-0.35771
Sr	0.46004	-0.10186	0.90859	0.04611	-0.35771	1.00000

Varimax Factor Pattern

Factors	1	2	3	4	5	6
Eigenvalues	3.084412	2.108519	0.606164	0.122817	0.045295	0.032793
Portion	0.514	0.351	0.101	0.020	0.008	0.005
Cum. Portion	0.514	0.865	0.967	0.987	0.995	1.000

	Factor 1	Factor 2	Factor 3	Factor 4	Factor 5
Resid	0.87695	-0.40457	-0.14472	0.17826	0.02686
Ca	-0.97243	0.06074	-0.14190	-0.11086	-0.03872
Mg	0.20730	-0.90183	-0.31453	0.06046	0.20281
Fe	0.95015	0.00494	0.14420	-0.27369	-0.03095
Mn	0.12352	0.26024	0.95702	-0.01597	-0.00716
Sr	0.06321	-0.98250	-9.11513	-0.01537	-0.12802

SODA DAM

Correlation Matrix

	Resid	Ca	Mg	Fe	Mn	Sr
Resid	1.00000	-0.79884	0.29150	-0.25390	0.11300	0.62624
Ca	-0.79884	1.00000	0.-5655	0.52664	-0.02037	-0.06584
Mg	0.29150	0.05655	1.00000	-0.24165	-0.56468	0.38204
Fe	-0.25390	0.52664	-0.24165	1.00000	0.79082	0.25869
Mn	0.11300	-0.02037	-0.56468	0.79082	1.00000	0.27264
Sr	0.62624	-0.06584	0.38204	0.25869	0.27264	1.00000

Varimax Factor Pattern

Factors	1	2	3	4	5	6
Eigenvalues	2.380748	1.979683	1.373534	0.247595	0.018439	0.000000
Portion	0.397	0.330	0.229	0.041	0.003	0.000
Cum. Portion	0.397	0.727	0.956	0.997	1.000	1.000

	Factor 1	Factor 2	Factor 3	Factor 4	Factor 5
Resid	-0.85147	0.00344	0.17548	-0.48945	0.06802
Ca	0.97802	0.16890	0.10850	-0.02200	0.05184
Mg	-0.00693	-0.25856	0.93302	-0.25010	0.00508
Fe	0.37812	0.91099	-0.04049	-0.13542	0.08454
Mn	-0.12850	0.88844	-0.40170	-0.15751	-0.08935
Sr	-0.14968	0.21609	0.21619	-0.94030	-0.00176

APPENDIX E

BEHAVIOR OF OTHER BIVALENT METALS IN CARBONATES

Strontium

Little study has been undertaken in regard to the behavior of strontium and its effect on the precipitation of $CaCO_3$ minerals under freshwater, subaerial conditions. However, substantial research has analyzed this factor in terms of marine carbonate sedimentation (Kulp et al., 1952; Thompson and Chow, 1955; Turekian and Kulp, 1956; Oxburgh et al., 1959; Siegel, 1961; Holland et al., 1963, 1964a; Bausch, 1965, 1968b; Kinsman and Holland, 1969a, 1969b; Veizer et al., 1971; Veizer and Demovic, 1974; Bathurst, 1975).

The high Sr/Ca- ratio (9.23) of sea water contrasts sharply with the low Sr/Ca- ratio (0.5 - 5.0) usually found in the freshwater environment (Odum, 1957; Irion and Müller, 1968b). Most investigators agree that the strontium concentration in marine sediments ranges from 100 ppm to 1200 ppm with an average value of 500 to 500 ppm Sr (Kulp et al., 1952; Vinogradov and Ronov, 1956). In contrast, freshwater carbonates contain slightly lower strontium levels on the average (<1000 ppm, Irion and Müller, 1968b). Some freshwater studies show surprisingly high strontium concentrations up to 3500 ppm (Kolesar, 1968; Müller, 1969a, 1971), but these values are unusual and rarely characteristic of a given environment.

Several variables influence the distribution of strontium found in carbonate rocks: crystal chemistry, age, salinity, clay mineral content, taxonomic level of organisms which include strontium in their framework, and environment of deposition. Some of these factors do not directly pertain to inorganic $CaCO_3$ precipitation in freshwater

conditions, but a general synopsis of all the factors involved is helpful in understanding the role of strontium.

Influencing Factors

Crystal Chemistry. Consideration of the two $CaCO_3$ polymorphs, calcite and aragonite, indicates that the aragonite lattice permits the substitution of appreciable amounts of Sr^{++} due to the fact that the large cations incorporated in the aragonite structure allow easier replacement to occur. The calcite structure admits smaller cations, and therefore the modification of the calcite lattice is less favorable for the incorporation of strontium. Distribution coefficients of aragonite/solution versus calcite/solution show that aragonite can absorb ten times the amount of strontium that calcite can under equal conditions (Oxburgh et al., 1959; Holland et al., 1963, 1964a, 1964b). In addition, aragonite is approximately sixteen times more soluble than calcite. Thus, one would expect high strontium aragonite to be a metastable constituent of geologically young materials. This relationship has been borne out in the geologic record quite convincingly. In recent marine sediments where aragonite is abundant (i.e., reef and lagoon areas), the strontium content is high; on the other hand, in basin sediments where calcite prevails, the strontium content is characteristically low. In fact, Siegel (1960) found that a linear relation exists where the strontium content decreases simultaneously with a decrease in the aragonite content.

Age. The age of carbonate rocks has a distinct influence on the strontium concentration present. As noted above, the significant loss of strontium with age is undoubtedly a direct result of the

aragonite-calcite transformation (Kahle, 1965). This relationship was tested by Vinogradov and Ronov (1956) on suites of carbonate rocks of the Russian platform; a satisfactory inverse linear correlation exists between increase in the strontium content and decrease in the geologic age of the formation.

Salinity. Sediment deposited under evaporitic conditions of high salinity shows distinctly high strontium concentrations (Vinogradov and Ronov, 1956). Müller (1962) states that this situation is the result of altered concentrations of sea water in evaporite formations and the high strontium content in anhydrite. Bausch (1968b) suggests plots of strontium content against insoluble residue content might prove helpful in recognizing limestones influenced by increased salinity.

Clay Content. Bausch (1965, 1968a) states that the strontium content of limestones can be related to the clay content. Because of strontium enrichment in the pore space during the aragonite-calcite transition, the clay minerals present can absorb unusual amounts of "free" strontium cations rejected in the aragonite dissolution. In order to accept this hypothesis, a nearly closed system with a small pore volume is assumed (Chave, 1960). This assumption would eliminate carbonates which have undergone extensive diagenesis or groundwater influx and effectively restrict this correlation technique to recent sediments.

Taxonomic Levels of Organisms. Certain organisms can increase their concentration of strontium by a factor of more than one thousand above that of the waters in which they live (Kulp et al., 1952; Thompson and Chow, 1955; Turekian and Armstrong, 1964; Friedman, 1968). In shelled organisms, this phenomenon is a function of the composition

of the shell material. Some genera (e.g., corals) have shells composed of high-strontium aragonite with strontium values usually above 100 ppm, while others (e.g., mollusks) construct their shells of low-strontium aragonite and consequently have lower strontium concentrations (Matthews, 1966; Friedman, 1968; Müller, 1968).

For recent specimens, the effectiveness of different moss or algal species on strontium intake is not well known. Irion and Müller (1968b) conducted studies on several varieties of mosses and algae associated with calcareous tufas from Germany. The low strontium values present were attributed to environmental characteristics and not biogenic modification.

Environment. Ultimately, the amount of strontium found in carbonate rocks reflects the strontium concentration of the water at the time of deposition. In the marine environment, this situation may be influenced primarily by the salinity of the depositional solution. On the other hand, under freshwater conditions the geologic and lithologic setting of the drainage area probably exerts greatest control on the amount of strontium present.

Dolomites

According to Weber (1964) and Bausch (1968b), dolomites consistently show lower strontium contents ($\overline{X}$ = 100 ppm) than pure limestones. This may be explained by the complete metasomatic replacement of this carbonate, which causes a further decrease in the trace element content.

Magnesium

Magnesium can occur in carbonates in a variety of forms.

These are: 1) ankerite, $CaFe(CO_3)_2$ (Usdowski, 1963; Brovkov, 1964); 2) magnesite or hydromagnesite, $MgCO_3$ and $Mg_4(OH)_2(CO_3)_3 \cdot 3H_2O$, respectively (Alderman and Von der Borch, 1960); 3) dolomite, $CaMg(CO_3)_2$ (Alderman and Von der Borch, 1960, 1963; Peterson et al., 1963; Skinner, 1963; Taft and Harbaugh, 1964); 4) high-Mg calcite, >11 mole % $MgCO_3$ (Stehli and Hower, 1961; Kübler, 1962; Siebold, 1962; Füchtbauer and Goldschmidt, 1964; Taft and Harbaugh, 1964); 5) low-Mg calcite, <5 mole % $MgCO_3$ (Fyfe and Bischoff, 1965; Berner, 1967). Since this study concerns primary inorganic $CaCO_3$ formation in the freshwater environment, discussion is restricted to the effect Mg^{++} has on calcite versus aragonite precipitation. In addition, consideration of marine versus non-marine environments and published values of Mg^{++} concentrations in selected freshwater carbonates will be analyzed.

During the inorganic precipitation of $CaCO_3$ minerals, Mg^{++} is the chief inhibitor in the growth of calcite over aragonite. Kitano (1962) evaporated solutions of $Ca(HCO_3)_2$ with and without various salts in the proportions in which these are found in sea water. In the presence of $MgCL_2$ only aragonite was formed, in its absence only calcite. Usdowski (1964) found that an increase in the Mg/Ca- ratio in a solution furthers the precipitation of aragonite rather than calcite.

The standard free energies of formation of pure calcite and pure aragonite are so close together (-269.7 kcal./mole and -269.5 kcal./mole, respectively), that small changes in the environment, such as the introduction of Mg^{++} into the solution, would be expected to have important consequences. Lippmann (1960) found that the difference in the standard free energies of formation of the hydrated Ca^{++} and Mg^{++} ions account for the reluctance of calcite to grow in aqueous solutions

containing Mg^{++}. He noted that $\Delta F°$ of hydration for Ca^{++} is -428 kcal./mole and for Mg^{++} -501 kcal./mole. As these hydrated ions assimilate at the surface of the crystal, Ca^{++} is more easily released from its water dipoles and joins $CO_3^{=}$ to construct the least soluble lattice, which is calcite. If the activity of Mg^{++} is high enough, the lattice constructed is magnesian-calcite. The Mg^{++} ions still hydrated are absorbed on the surface of the nucleus. However, the work that must be done to dehydrate them is such that the ΔF_f° of aragonite (which holds very little Mg^{++}) is, in these circumstances, greater than for magnesian-calcite. So aragonite crystals grow while the growth of calcite nuclei is prevented by the obstructed adsorption of hydrated Mg^{++}. These findings by Lippmann support similar conclusions by Davies and Jones (1955) and are buttressed by the more recent work of Bathurst (1968).

Müller (1969a) contends that the controlling factor of primary carbonate species formation is the value of the Mg/Ca- ratio of the precipitating solution. Studies conducted on lacustrine sediments and speleothems from selected areas in Europe and Asia yielded the following generalized information in regard to the carbonate precipitate in terms of Mg/Ca- ratios:

1) Mg/Ca- ratio <2 low-Mg calcite

2) Mg/Ca- ratio 2-12 high-Mg calcite (+aragonite)

3) Mg/Ca- ratio >12 aragonite

Müller states that these values may be universally applied to any freshwater carbonates where Mg/Ca- ratio and water volume maintain near constant rates (Müller et al., 1972).

The only significant difference in the inorganic carbonate mineralogy between the non-marine and marine environments is that low-Mg calcite does not form under marine conditions. The explanation is that the high Mg/Ca- ratio of sea water (near 5.0) does not allow formation of low-Mg calcite. In addition, primary carbonate precipitation under freshwater conditions allows a variety of precipitates to form due to the fact that Mg/Ca- ratios are so variable. The near constant Mg/Ca- ratio in sea water, however, limits the carbonate species to aragonite or high-Mg calcite under usual conditions.

Data on the magnesium content of freshwater carbonates is scarce. Müller (1969a, 1972) and his associates have gathered the greatest volume of data on this subject and he has found Mg^{++} contents to vary from 0 to 1200 ppm depending upon the environment of deposition in which they are found. In particular, Mg^{++} content of tufas in Germany varies between 240 ppm and 1060 ppm with an average value of 462 ppm. This work suggests guidelines for typical magnesium contents in similar environments.

Iron

The formation of iron minerals is a function of the Eh-pH and partial pressure under which they are deposited. The variables of total iron concentration, activities of dissolved carbonate and sulfur, and temperature, influence the range of the different mineral stability fields. For purposes of the present study, depositional environment allows calculations based on 25° C and 1 atm total pressure; activities of pure solids and pure liquids are taken to be unity, and activity of a gas phase is assumed to be equal to its pressure. Although elevated

temperatures are encountered in many freshwater systems (i.e., thermal springs), analytical variations are minimal under these modified conditions.

Calculations for the total replacement of calcite ($CaCO_3$) by siderite ($FeCO_3$) should follow the equation

$$CaCO_3 + Fe^{++} \rightleftharpoons Ca^{++} + FeCO_3$$

for which the equilibrium constant is

$$K = \frac{(Ca^{++})}{(Fe^{++})} = \frac{(Ca^{++})\ (CO_3^{=})}{(Fe^{++})\ (CO_3^{=})} = \frac{4.5 \times 10^{-9}}{3.0 \times 10^{-11}} = 150.$$

This means that calcite should be replaced by siderite if it is in contact with a solution containing Fe^{++} in a concentration more than 1/150 that of Ca^{++}, and likewise that siderite can be replaced by calcite only if the solution contains more than 150 times as much Ca^{++} as Fe^{++}. Under the conditions of freshwater carbonate precipitation, however, the amounts of iron that theoretically could be present in solution are mostly below 0.01 ppm (Hem and Cropper, 1959); a concentration much too negligible for appreciable iron-rich carbonate formation. Furthermore, due to the oxidizing environment present, any iron in solution is immediately liberated as ferric oxide or hydroxide before substitution of Fe^{++} for Ca^{++} in the carbonate lattice is possible (Lippman, 1973).

Formation of iron carbonate is highly unlikely under conditions of oxidizing freshwater precipitation. Assuming a high total carbonate (1 M) and low total sulfur (10^{-6} M) content for calculations, an Eh-pH diagram encompassing ordinary freshwater subaerial deposition is

shown in Fig. 40. The stippled region represents redox conditions pertinent to the present investigation. As interpreted from the diagram, siderite has two fields of stability separated by the field of pyrite. The occurrence is practically restricted to neutral and basic solutions; it can precipitate from weakly acid solutions only if the concentration of dissolved iron is abnormally high. As temperature increases (>100° C) or at higher sulfur concentrations, the pyrite and hematite stability fields would expand at the expense of the siderite field.

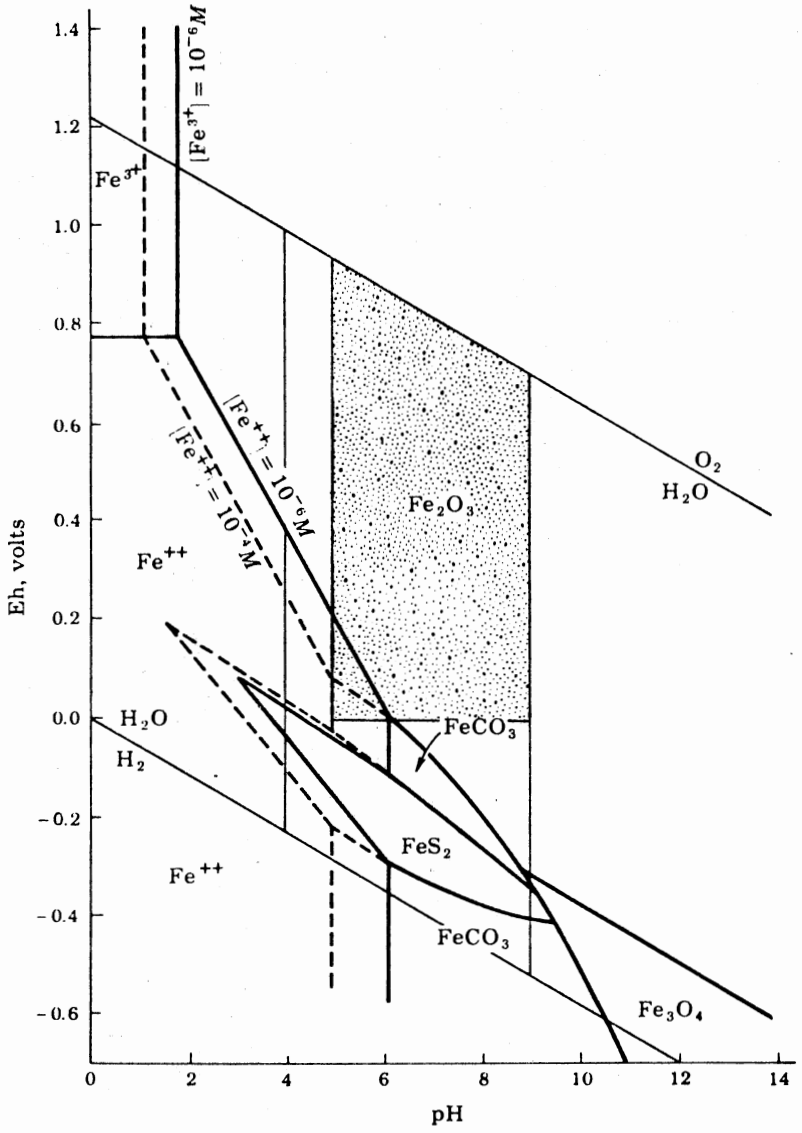

Fig. 40.-Eh-pH diagram showing stability fields of common iron minerals. Total activity of dissolved carbonate, 1M, of dissolved sulfur, 10^{-6}M. Solid field boundaries on left side of diagram are for total dissolved iron = 10^{-6}M, dashed lines for 10^{-4}M. Stippled area represents conditions of freshwater carbonate formation. Modified after Krauskopf, 1967.

VITA

William Richard Trent

Candidate for the Degree of

Master of Science

Thesis: SOME ASPECTS OF THE PETROLOGY AND GEOCHEMISTRY OF SELECTED FRESHWATER CARBONATES

Major Field: Geology

Biographical:

Personal Data: Born in Kansas City, Missouri, January 23, 1954, the son of Mr. and Mrs. Richard A. Trent. Married Patricia L. McGuire, June 11, 1977.

Education: Graduated from Rockhurst High School, Kansas City, Missouri, in May, 1972; received Bachelor of Science degree in Geology from University of Missouri at Kansas City, in May, 1976; completed requirements for Master of Science degree at Oklahoma State University in July, 1978, with a major in Geology.

Professional Experience: Junior member of the American Association of Petroleum Geologists; teaching and research assistant, University of Missouri at Kansas City, August, 1974 - May, 1976; teaching assistant, Oklahoma State University, August, 1976 - May, 1977; assistant instructor, Oklahoma Geology Field Camp, May, 1977 - June, 1977; research assistant, Oklahoma State University, July, 1977; Amoco Production Company fellowship, 1977-1978; production geologist, Thomas N. Berry & Company, 1977-1978.